Miocene extension and magma generation in the Apuseni Mts. (western Romania): a review

Ioan Seghedi, Theodoros Ntaflos, Zoltan Pécskay, Cristian Panaiotu, Viorel Mirea & Hilary Downes

View supplementary material

Published online: 26 Aug 2021.

Submit your article to this journal

Article views: 44

View related articles

View Crossmark data

Taylor & Francis
Taylor & Francis Group

Check for updates

REVIEW ARTICLE

Miocene extension and magma generation in the Apuseni Mts. (western Romania): a review

Ioan Seghedi [iD][a], Theodoros Ntaflos [iD][b], Zoltan Pécskay [iD][c], Cristian Panaiotu [iD][d], Viorel Mirea [iD][a] and Hilary Downes [iD][e]

[a]Institute of Geodynamics "Sabba S. Stefănescu", Romanian Academy, Bucharest, Romania; [b]Department Of Lithospheric Research, University Of Vienna, Vienna, Austria; [c]Isotope Climatology And Environmental Research Centre (ICER), Institute For Nuclear Research, Hungarian Academy Of Sciences, Debrecen, Hungary; [d]Paleomagnetic Laboratory, University Of Bucharest, Bucharest, Romania; [e]Department Of Earth And Planetary Sciences, Birkbeck University Of London, London, UK

ABSTRACT

The Apuseni Mts. is a key area to study the interplay between intra-continental extensional tectonics, sedimentation, and magmatism. These events occurred from ~14.5 to 7 Ma, covering the collision of the Tisza-Dacia mega-unit with the East European Platform at ~11 Ma and formation of a thin-skinned fold-thrust belt in the East Carpathians. The Zărand-Brad-Zlatna basin (~120 km in length) is the main graben system associated with the magmatic activity. To its south, it is bounded by two younger (<12 Ma) sub-basins: Caraci and Săcărâmb both hosting active magmatism. To the north-east, the smaller Roşia Montană–Baia de Arieş–Bucium sub-basin and, to the south-east, the Deva sub-basin are also associated with magmatism. Several andesite intrusions are also known in the northernmost Apuseni Mts. at Moigrad. Volcanism from ~14.5 to ~12 Ma displays a typical calc-alkaline affinity with high $^{208}Pb/^{204}Pb$ (38.6–38.8) and $^{207}Pb/^{204}Pb$ (15.65–15.67), moderate to high $^{87}Sr/^{86}Sr$ (0.7047–0.7085) and low to high $\delta^{18}O_{wr}$ (>7‰) values. The younger igneous rocks (<12 Ma) show high Sr/Y and a variable but significant enrichment in LILE up to ~7 Ma, coupled with low $^{87}Sr/^{86}Sr$ (0.7040–0.7045), low $^{208}Pb/^{204}Pb$ (38.2–38.6) and $^{207}Pb/^{204}Pb$ (15.59–15.63), and low $\delta^{18}O$ (5.5–5.7‰). The geodynamic evolution of the area started as regional transtensional with rotational tectonics generating horst and graben structures and ended with a transpressional event. This setting provided the conditions for the formation of a large underplated magma chamber at the crust – mantle boundary (MASH zone), in response to hot upwelling convective asthenosphere. Melting of the lower crust and mixing with mantle melts may have played an important part in the magmatic evolution. The spatial and temporal changes in composition were generated in magma at the crust – mantle boundary, with different crustal thicknesses. Further crustal assimilation and minor fractional crystallization in crustal magma chambers were characteristic for each region.

1. Introduction

The Alpine-Himalayan collision system is marked by scattered and discontinuous igneous activity, mostly post-dating the diachronous continent–continent collisional. This magmatism involves melt generation from both mantle and crustal sources (e.g. Lustrino *et al*. 2011; Prelević and Seghedi 2013; Chung *et al*. 2005; Niu *et al*. 2013), with overall geochemical characteristics resembling magmas generated in subduction systems (Seghedi *et al*. 2004; Dilek and Altunkaynak 2009; Ersoy and Palmer 2013). In spite of the wealth of data for these igneous rocks, understanding of the petrogenetic processes and the extent of crustal involvement remains controversial (e.g. Hu *et al*. 2017; McNab *et al*. 2018; Uslular and Gençalioğlu-Kuşcu 2019; Rabayrol *et al*.

2019). An approach trying to link geodynamic processes (e.g. continent–continent collision; extensional post-collisional processes) with the geochemical 'response' of various sources (mantle/crust) may help in unravelling the complex interplay between tectonic and magmatic processes. Here we review the Miocene volcanism in the Apuseni Mts., one of the largest and most complex magmatic districts within the Carpathian-Pannonian region, situated ~200 km away from any identified Miocene subduction system (e.g. Linzer 1996; Ustaszewski *et al*. 2008; Schmid *et al*. 2008, 2020; Van Hinsbergen *et al*. 2020). In this work, we interpret all available geochemical, petrological, and geochronological data, and complete these with some new results for volcanic areas not yet discussed, including some special

petrographic types (e.g. garnet-bearing and Roşia Montană rocks), to obtain the broadest possible picture. Our aim is to improve the understanding of magmatism in extensional intracontinental orogenic systems in general.

This review incorporates studies of the geological setting (e.g. Săndulescu 1988; Balintoni and Vlad 1998; Seghedi *et al.* 1998, 2004; Csontos and Vörös 2004; Neubauer *et al.* 2005; Seghedi and Downes 2011) and the geochronology, petrography, mineralogy, whole-rock geochemistry, and Sr-Nd-Pb-O isotopic characteristics of the Miocene magmatic products (Downes *et al.* 1995; Pécskay *et al.* 1995, 2006; Roşu *et al.* 2004; Kouzmanov *et al.* 2003, 2005, 2006, 2007; Hindson 2009; Seghedi *et al.* 2004, 2007, 2008, 2010; Tschegg *et al.* 2010; Harris *et al.* 2013; Gallhofer 2015; Supplemental online Table S 2.2). It also presents new geochemical and K-Ar data (Supplemental online Table S1 and S 2.1).

2. Location

The Carpathian orogenic belt resulted from oblique convergence during orogenic subduction and continent–continent collision that drove the ALCAPA (ALpine-CArpathian-PAnnonian) and Tisza (also known as Tisia)–Dacia Mega-Units into the Carpathian embayment, a bay area close to the stable East-European /Moesian domain (e.g. Săndulescu 1988; Csontos 1995; Schmid *et al.* 2008, 2020). This convergence resulted in large-scale tectonic deformation and rotations in the interior of the Carpathians and formation of several extensional basins (e.g. Horváth 1993; Csontos 1995; Fodor *et al.* 1999; Horváth *et al.* 2015; Balázs *et al.* 2016).

The Apuseni Mts. are located ~200 km behind the present-day collision front of the Carpathians. They are considered to be a relic of a wider and continuous mountain chain between the Dinarides and the Carpathians formed at the end of the Palaeogene (Maţenco 2017). During the Middle Miocene, extension occurred in the Pannonian Basin coupled with magmatic activity in the Apuseni Mts., which continued until the Late Miocene (Roşu *et al.* 1997, 2004; Seghedi *et al.* 2004). This magmatism was followed by the formation of several small basins in the eastern part of the Great Hungarian Plain towards the Apuseni Mts., which are characterized by half-graben geometries, arcuate shapes, and NW-SE strikes (from north to south: Derecske-Borş-Borod, Beiuş, Békés-Grăniceri-Zărand; e.g. Săndulescu 1988; Balázs *et al.* 2016; Figure 1a). The basin structures were formed as low-angle detachments with footwall exhumation controlling half grabens that exhumed deep crustal rocks (Tari *et al.* 1999; Fodor et al.

1999; Csontos and Nagymarosy 1998; Balázs *et al.* 2016). However, with the exception of the Derecske basin, the footwalls of such structures along the western margin of the Apuseni Mts. are unmetamorphosed. Sedimentary infill in these extensional grabens varies from a few tens of metres up to a few km (e.g. Horváth *et al.* 2006). Below the largest Békés-Zărand basin, upwelling of the asthenospheric mantle to 40–45 km depth has been inferred from geophysical observations and numerical modelling (Tari *et al.* 1999; Balázs *et al.* 2017).

Based on their different pre-Alpine geological evolution (e.g. Ianovici *et al.* 1969, 1976; Bleahu *et al.* 1981; Săndulescu 1984; Balintoni 1994, 1997; Dallmeyer *et al.* 1999; Pană *et al.* 2002; Schmid *et al.* 2008, 2020; Balintoni *et al.* 2010), two main structural units have been recognized in the Apuseni Mts.: North Apuseni and South Apuseni (Figure 1a).

From a geotectonic point of view, the Apuseni Mountains are located at the contact between the merged Tisza and Dacia continental microplates (Figure 1a). The South Apuseni comprises Jurassic Transylvanian ophiolitic nappes (equivalent of the East Vardar ophiolites), which according to Schmid *et al.* (2008) overlie the Dacia Unit. Schmid *et al.* (2008) attributed the Biharia Nappe System to the Dacia Unit based on the fact that the Transylvanian Ophiolitic Nappes (e.g. Savu 1996; Saccani *et al.* 2001; Bortolotti *et al.* 2002; Nicolae and Saccani 2003; Hoeck *et al.* 2009; Ionescu *et al.* 2009; Gallhofer 2015) overlie the Bucovinian Nappe System and the Biharia Nappe System (e.g. Săndulescu 1984; Krézsek and Bally 2006). However, other authors (e.g. Csontos and Vörös 2004; Haas and Péró 2004) previously considered it to be an integral part of Tisza. Gallhofer *et al.* (2017) proposed a geodynamic evolution in which the Late Kimmeridgian (150–153 Ma) was the maximum age of emplacement of the South Apuseni ophiolites and associated granitoids onto the Dacia Unit. An Albian to Turonian age (110–90 Ma) was proposed for the main deformation that formed the present-day geometry of the Apuseni nappe stack, which also led to a pervasive retrograde greenschist-facies overprint (Reiser *et al.* 2016).

Late Cretaceous basins (with Gosau-type sediments; Schuller *et al.* 2009) unconformably developed over all the tectonic units after the Late Cretaceous convergence and were intruded by coeval calc-alkaline magmas (e.g. Berza *et al.* 1998; Gallhofer *et al.* 2015; Vander Auwera *et al.* 2015). The post-Palaeocene tectonic uplift of the Apuseni Mts. area interrupted sedimentation until Early-Middle Miocene. The Miocene evolution of the Apuseni Mts. is related to brittle tectonics (Săndulescu 1988), marked mainly by complex extensional graben-like structures, which opened along the western edge of
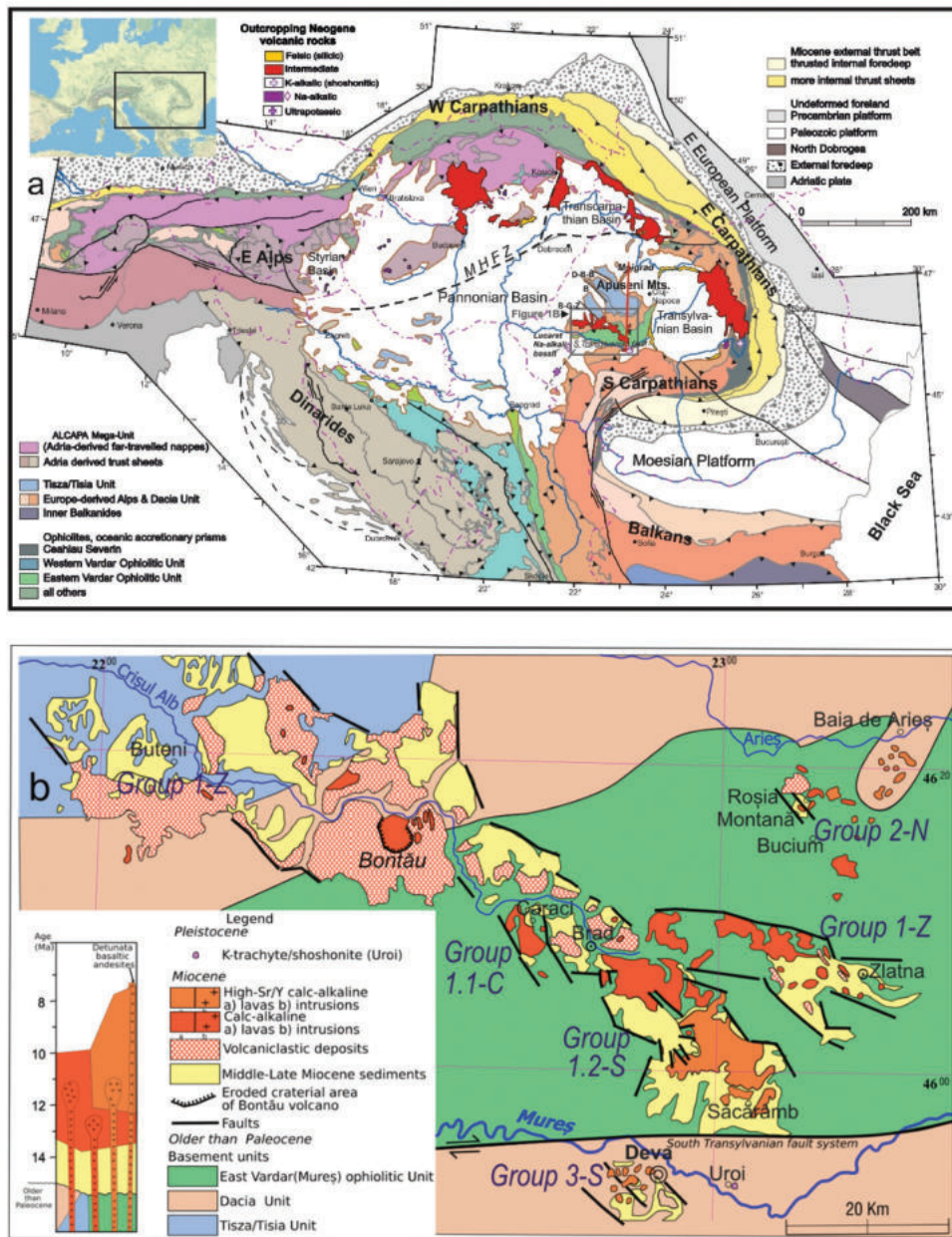
Figure 1. *A) Sketch map of the Carpathian – Pannonian region (simplified after* Schmid *et al.* 2008) *showing the Miocene – Quaternary magmatism (simplified after* Pécskay *et al.* 2006) *with late Miocene – Quaternary sedimentary cover;* Figure 1b *in a frame; Moigrad occurrences are north of the Apuseni Mts.; MHFZ – Mid Hungarian Fault; D-B-D – Derecske-Borş-Borod, B – Beiuş and B-G-Z – Békés-Grăniceri-Zărand grabens;Lucareţ Pleistocene alkali basalts are shown; the red vertical line indicate the profile in the* Figure 13; *b) Sketch of Miocene magmatic rock occurrences in the NW-SE graben structures in the South Apuseni Mts., separated into main Zărand-Brad-Zlatna (Group 1-Z) graben-type basin and several sub-basins Caraci (Group 1.1-C), Săcărâmb (Group 1.2-S), Roşia Montană – Baia de Arieş area (Group 2-N) and Deva (Group 3-S), after the Geological map of Romania (1:1,000,000). A simplified stratigraphic column showing lithologies and ages studied and discussed in text is given.*

the Apuseni Mts. (e.g. Csontos 1995; Balázs *et al.* 2016). From the Badenian (Serravalian in Standard Chronostratigraphy) onwards, the Apuseni Mts. remained as a high relief segment after the general subsidence of the Pannonian Basin and Transylvanian Basin. Recent models of crustal structure that cover all the western part of Romania, based on multiple

geophysical methods, suggest a variable Moho depth of 24–28 km in the Zărand basin and more than 35 km in the Deva area (Bala *et al.* 2017). Development of Neogene volcanism followed the extension and formation of the Middle Miocene sedimentary strata in the Zărand Basin (e.g. Ghiţulescu and Socolescu 1941; Ianovici *et al.* 1969 and references therein). Radiometric

ages and magnetic polarity data are in agreement with biostratigraphy (Pécskay *et al.* 1995; Roşu *et al.* 1997, 2004).

Miocene magmas did not pierce all the NW-SE striking grabens at the western margin of the Apuseni Mts., but mainly the Zărand-Brad-Zlatna basin and several small wedge-like basins connected to the south of the Zărand-Brad-Zlatna, such as the Caraci (Jude *et al.* 1973) and Săcărâmb sub-basins (e.g. Bleahu *et al.* 1981; Neubauer *et al.* 2005; Figure 1b). Magmatism also occurred in several other small grabens in the central part of Apuseni Mts., towards the north in the Roşia Montană – Baia de Arieş area (Ilie 1958) and south, in the Deva area, where the volcanic structures and sub-volcanic-hypabyssal intrusions cluster as isolated bodies (e.g. Boştinescu and Savu 1996; Figure 1b). Middle–Late Miocene shallow marine to lacustrine sediments fills all these basins (Bleahu *et al.* 1981; Balintoni and Vlad 1998; Csontos *et al.* 2002; Figure 1b). Several isolated andesitic shallow intrusions are situated in North Apuseni at Moigrad (e.g. Roşu *et al.* 2004; Figure 1a). The igneous rocks discussed here will be separated according to their affiliation with the basin system in which they occur as follows: Group 1-Z for the Zărand-Brad-Zlatna basin, the main graben system; Group 1.1-C and 1.2-S representing the two smaller south-directed wedge sub-basins, Caraci and Săcărâmb; Group 2-N for the north-eastern Roşia Montană–Baia de Arieş–Bucium basin system and Group 3-S for the south-east Deva basin system. Moigrad rocks are represented by one sample.

The magmatism is typical subalkaline and interpretations generally assumed that it was generated by decompression melting during extension (e.g. Roşu *et al.* 2004; Seghedi *et al.* 2004) of a mantle source that had been metasomatized during an older subduction event (e.g. Cretaceous; Harris *et al.* 2013). This is in agreement with structural observations, which indicate that the onset of extension began in Middle Miocene (i.e. ~16 Ma). Subsequent normal faulting and further activation of listric normal faults and clockwise rotation of the hanging walls coeval with the main collapse phase of the Pannonian Basin are recorded also during the upper part of the Middle Miocene (e.g. Dinu *et al.* 1991; Csontos 1995; Balázs *et al.* 2016).

Roşu *et al.* (2004) and Harris *et al.* (2013) described a temporal transition from typical calc-alkaline to adakite-like calc-alkaline rocks and considered them as related to magmas favoured by increased extension and increasing degrees of partial melting of a metasomatized mantle/lower crust heterogeneous source, which was isotopically depleted but enriched in incompatible elements. The extensional regime associated with asthenospheric upwelling was ascribed to

the eastward translation and fast clockwise rotation of the Tisza-Dacia Mega Unit during Middle Miocene times (e.g. Roşu *et al.* 2004; Seghedi *et al.* 2004).

Pleistocene eruptions of intraplate alkalic basaltic magmas with an asthenospheric origin (ocean-island basalt (OIB)-like) occurred under local extension along the South Transylvanian fault system in the South Apuseni Mts (e.g. Downes *et al.* 1995; Tschegg *et al.* 2010) but are only considered in this study as an example of a local genuine asthenosphere-derived magma.

3. Volcanological outline

Miocene magmatic rocks occur in both volcanic and intrusive subvolcanic forms in the Apuseni Mts. The westernmost volcanic rocks cropping out in the Zărand Basin form isolated lava domes and volcaniclastic deposits belonging to the strongly eroded composite Bontău volcano (Seghedi *et al.* 2010; Figure 1b). Towards the south-east sector, the eroded complex volcano of Caraci developed into a small wedge-like basin linked to the Zărand basin. Its central part is a dome extrusion of basaltic andesite composition, surrounded by older andesitic lava flows and volcaniclastic deposits cut by dykes and vent breccia (Jude *et al.* 1973).

Multiple clustered volcano-intrusive complexes crop out from Brad to Zlatna. The same holds for the younger (<12 Ma) associated Săcărâmb wedge-shaped sub-basin to the south, which trends NNW-SSE. The other two small sub-basins, Roşia Montană – Baia de Arieş – Bucium and Deva, are characterized by individual effusive volcanic centres and/or intrusive bodies (Figure 1b).

Numerous small-sized intrusive bodies (metres up to hundred metres) occur, including dykes, sills, microlaccoliths, and intrusive breccias. Some of them likely represent the roots of volcanoes that were dominated by lavas and dome structures (Lexa *et al.* 2010). Magmatic activity in the Apuseni Mts. was characterized by both low-frequency and low-output rate. Since magmatism was active over a time span of 7 Myr (~14.5–7 Myrs), it can be assumed that the long-lived Miocene rift graben system experienced stepwise changes in fracture propagation that promoted repeated dyke intrusion to generate numerous mostly small-sized volcanic forms.

4. Eruptive history

Miocene magmatic activity developed between 14.6 and ~7 Ma, based on whole-rock K-Ar (Pécskay *et al.* 1995; Roşu *et al.* 1997, 2004) and zircon dating (Kouzmanov *et al.* 2003, 2005, 2006, 2007) (Figure 2a). Recently reported U-Pb zircon ages (e.g. Holder 2016; Brunner *et al.* 2018; Ene *et al.* 2019) are mostly in agreement
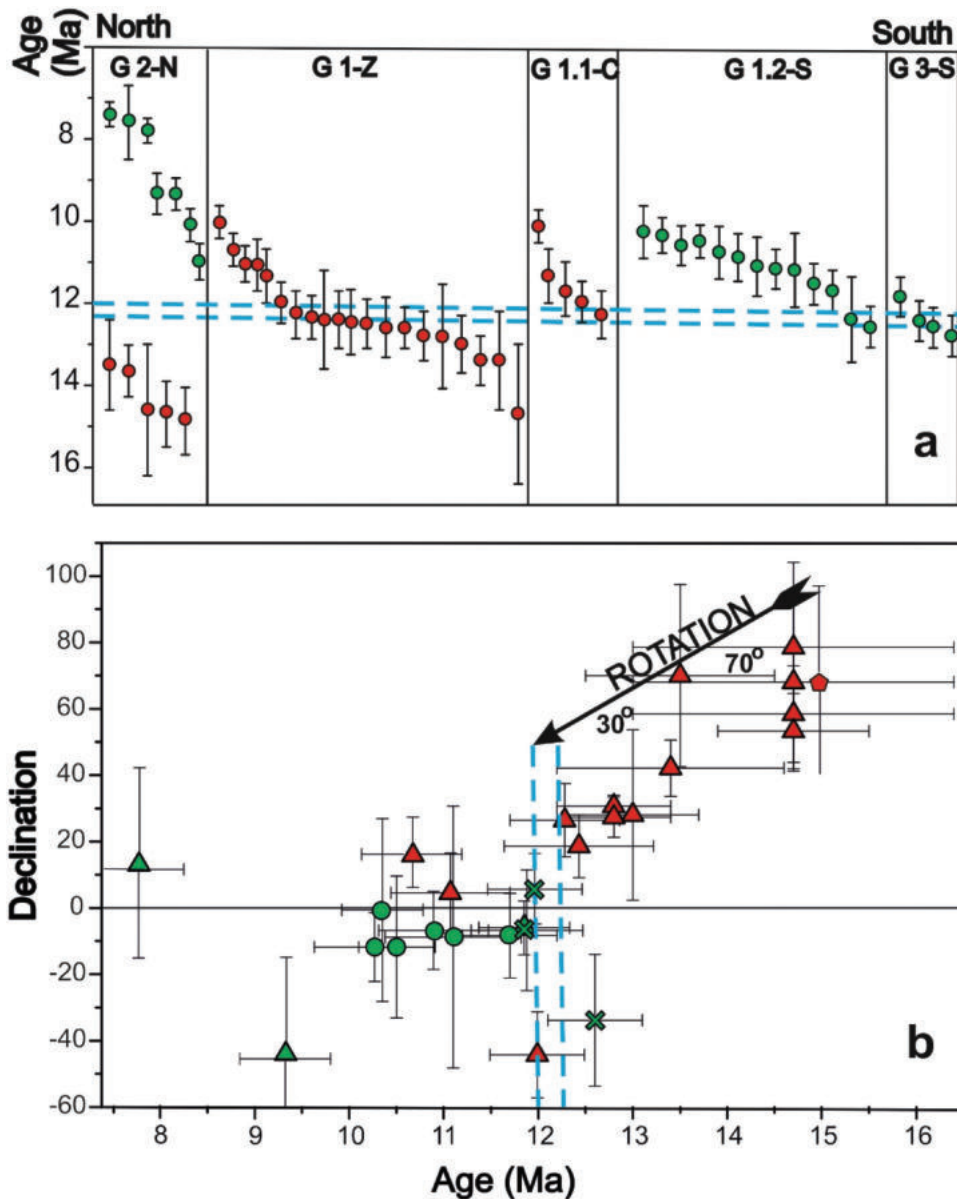
Figure 2. *A) Time evolution of volcanic activity in the South Apuseni Mts. for the various basins and sub-basins: from North to South: Roşia Montană-Baia de Arieş-Bucium (Group 2-N) sub-basin; Zărand-Brad-Zlatna (Group 1-Z) basin; Caraci (Group 1.1-C); Săcărâmb (Group 1.2-S) and Deva (Group 3-S) sub-basins. Dashed line marks the end of clockwise rotations at 12.1–12.3 Ma; b) Palaeomagnetic declination versus age for igneous rocks sampled both for palaeomagnetism and K–Ar ages (Roşu et al. 2004; this study). For each site the error bars for both palaeomagnetic declination and age are shown. The arrow marks the period of clockwise tectonic rotation. Symbols: Filled red pentagon-Group 2-N; Filled red triangles-Group 1-Z; fill green circle-Group 2-N; filled green triangles: Group 2-N; Green crosses: Group 3-S. The red symbols in both a) and b) panels denote typical calc-alkaline rocks and the green symbols are high-Sr/Y calc-alkaline rocks. The new data complete and strengthen the previous results.*

with the K-Ar data, but occasionally yield younger ages. Based on the K-Ar dates and palaeomagnetic data, an initial 70° clockwise block rotation of Tisza–Dacia occurred between 15 and 13 Ma, followed by a further 30° rotation at ~12.1 to 12.3 Ma that coincided with development of the NW-SE graben in the main Zărand-Brad-Zlatna basin. This was a period of typical calc-alkaline magma generation (Figure 2b; Panaiotu 1998; Pătraşcu et al. 1994; Roşu et al. 2004). As rotations ended

at ~12 Ma, further high Sr/Y calc-alkaline magmas were generated (Roşu et al. 2004), but also typical calc-alkaline magmas (e.g. Caraci and Bontău volcanoes; this study). Between ~12 and 10 Ma, and at the end of volcanic activity at ~8 Ma, volcanism developed in wedge-like graben structure formed along the southern part of the Zărand-Brad-Zlatna basin, which shows the development of en-echelon faulting related to the end of block rotations (Seghedi et al. 2004; Roşu et al. 2004; Neubauer

et al. 2005). In the Zărand-Brad-Zlatna, high Sr/Y calc-alkaline magmas are absent, and magmatic activity ceased at ~10 Ma with the final products of the Bontău and Caraci volcanoes (Jude *et al.* 1973; Seghedi *et al.* 2010; this study, see Supplemental online Table S1).

The most complex area, where active magmatism occurred over the longest time interval, is the northern-most Roşia Montană – Baia de Arieş area (~14.6–7 Ma). Here, typical calc-alkaline activity was followed by high-Sr/Y calc-alkaline magmatism and finally by emplacement of the least evolved products of the entire district, the two Detunata basaltic andesite necks (e.g. Roşu *et al.* 2004; Harris *et al.* 2013).

5. Petrography and classification

5. 1. Petrography

Miocene igneous rocks from the Apuseni Mts. are predominantly amphibole- and pyroxene-bearing andesites, though there are small volumes of basaltic andesites and dacites. Approximately 120 samples have been selected from the analysed and published in previous studies and 17 samples are new data (Supplemental online Table S2.1 and S2.2).

5.1.1 Basaltic andesites
Basaltic andesites occur as intrusion in the Detunata hills or lavas in the Bontău volcano. Basaltic andesites are either strongly porphyritic (clinopyroxene as phenocrysts) or aphyric (e.g. Detunata; Caraci dome), with 40–70 vol. % of microphenocrysts. Plagioclase is the dominant phase. Clinopyroxene is the principal mafic mineral. There are also orthopyroxene and olivine (only at Detunata) and rare amphibole (<5%). Plagioclase microphenocrysts are smaller in size (<0.2 to 3 mm) with respect to clinopyroxene and amphibole ones, and commonly show sieve-textured cores and rare oscillatory zoning. Clinopyroxene phenocrysts are very variable both in modal abundances (20–40 vol.%) and in grain size, with the largest phenocrysts being 5 mm. Clinopyroxene crystals occur in aggregates or rarely with amphibole, and contain inclusions of opaque minerals, apatite, and plagioclase. Amphibole microphenocrysts vary in size from <0.5 mm up to 5 mm in length, ranging from <1 to 5 vol. %. All amphibole microphenocrysts have opaque reaction rims or are completely pseudomorphed. Orthopyroxene shows variable abundance (1–5%) ranging in size from 0.2 to 2 mm. Most crystals are surrounded by reaction rims of clinopyroxene and opaques. Olivine is rare, occurring solely in Detunata basaltic andesites. The largest olivine is ~3 mm in size. The groundmass is glassy and contains fine-grained (<0.01 mm) aggregates of plagioclase, clinopyroxene, and opaques.

5.1.2 Andesites
Andesite is the most common and volumetrically dominant rock type. Andesites display a wide spectrum of varieties and occur in all the areas. Two-pyroxene varieties prevail in the west (Group 1-Z and 1.1-C), whereas amphibole- and biotite-bearing varieties mostly crop out in the east (all areas). The amphibole–pyroxene andesites occur all over. The rocks are slightly to strongly porphyritic, with a phenocryst assemblage dominated by plagioclase, followed either by pyroxene (clinopyroxene and orthopyroxene) or amphibole and lesser biotite. The phenocrysts are up to 1 cm in maximum dimension, with an average size between 3 and 5 mm, with abundances from 20 to 70 vol. %. All plagioclase phenocrysts show well-developed polysynthetic twinning and only few show zoning; some crystals have distinctive outer or inner resorption zones surrounded by clear rims, while others have sieved altered cores densely clouded by very fine grained (<0.02 mm) phyllosilicates and opaques. In the two-pyroxene varieties, clinopyroxene and orthopyroxene are present in equal amounts and are the dominant phenocryst phases (<0.05 to 2 mm in size), while in the amphibole- and biotite-bearing andesites clinopyroxene prevails. Amphibole is a major phenocryst phase; reddish brown or dark green in colour and ranging in size from <0.05 (microphenocrysts) to 7 mm (phenocryst). Crystals often have dark brown oxidized margins or altered/resorbed cores. Biotite is present as isolated flakes up to 1 mm in length in rocks from the eastern areas. Opaque minerals are generally <0.3 mm in size, and rarely up to 0.6 mm. The groundmass is rich in microlites (plagioclase, clinopyroxene, orthopyroxene) and glass. Amphibole ± clinopyroxene ± biotite andesite varieties are moderately to strongly porphyritic and have plagioclase, amphibole, rare clinopyroxenes, biotite and sporadic corroded quartz as phenocrysts and accessory, apatite, zircon, and Cr-spinels in the groundmass. Amphibole and biotite are partially oxidized. A small andesite occurrence considered previously as a trachyandesite (Roşu *et al.* 2004) belongs to this variety (samples 395 and 776/ZM-04-CH-13 in Supplementary table S 2.2).

5.1.3 Dacites
Dacites occur in the Group 1-Z, Group 2-N at Roşia Montană and Bucium and in the Group 1.2-S and show mineralogical characteristics similar to the amphibole-biotite andesites. However, the dacites display more strongly porphyritic textures (with phenocryst loads of 60–70 vol. %). They include plagioclase (sometimes

partially hydrothermally altered to phyllosilicates), quartz (with up to 2 cm length idiomorphic crystals at Roşia Montană volcano), amphibole, biotite, and rare clinopyroxene, as phenocrysts. Accessory minerals such as opaque minerals, apatite, and zircon occur in a microgranular or glassy groundmass. Rare garnet-bearing varieties can be found only in the Group 1-Z, where some of the rocks show a secondary hydrothermal alteration (propylitic) in the form of chlorite on amphibole or clinopyroxene.

5.2. Classification

The Miocene effusive/shallow intrusive rocks in the Apuseni Mts. range from basaltic-andesites to dacites (Figure 3; Roşu et al. 2004; Seghedi et al. 2007; Harris et al. 2013; data sources are given in Supplemental tables S1 and 1.1). The Roşia Montană rocks are andesite to dacite (Group 2-N, >12 Ma), garnet-bearing dacites (Group 1-Z) and the basaltic andesites and andesites in Group 1.1-C, published here for the first time (Supplemental online Table S2.1). The magmatic rocks were classified using classical diagrams of Na_2O+K_2O and K_2O vs. SiO_2 (Figure 3) (Peccerillo and Taylor 1976; Le Bas et al. 1986). They correspond to calc-alkaline series and are dominantly andesites with lesser basaltic andesites and dacites. There are a few rocks from the Groups 1.2-S, 2-N (<12 Ma), and 3-S that are richer in alkalis, and fall in the high-K calc-alkaline

classification. The main trend follows the recognized average crustal composition from the lower crust (LC) to upper crust (UC) (Rudnick and Gao 2003).

There are few small volcanoes of Pleistocene age at the southern part of Apuseni Mts which cover a wider affinity from Na-alkalic, K-alkalic to ultra-K alkaline (trachybasalts, trachyandesite/trachydacite, and tephriphonolite), and are clearly distinct from the Miocene rocks (Figure 1 a). These rocks, with the exception of trachybasalts, are not included for comparative purposes in this review, as their composition and origin have been discussed elsewhere (e.g. Seghedi et al. 2008; Seghedi and Downes 2011).

6. Geochemistry

6.1 Major and trace element data

With the exception of CaO and Fe_2O_3 and roughly K_2O, most of the Harker diagrams do not show good correlations (Figure 4). Among them, most rocks in Groups 2-N, 1.2-S and 3-S show higher alkali and P_2O_5 contents. There is an overall decrease of Fe_2O_3, CaO, and MgO, and to a lesser extent of TiO_2 and P_2O_5, and a slight increase of K_2O and an increasing variability of Na_2O with increasing SiO_2. The Al_2O_3 data are more scattered, but there is a negative correlation for the Group 2-N rocks. With the exception of MgO, Al_2O_3 and P_2O5, the Miocene Apuseni Mts. rocks lie between average
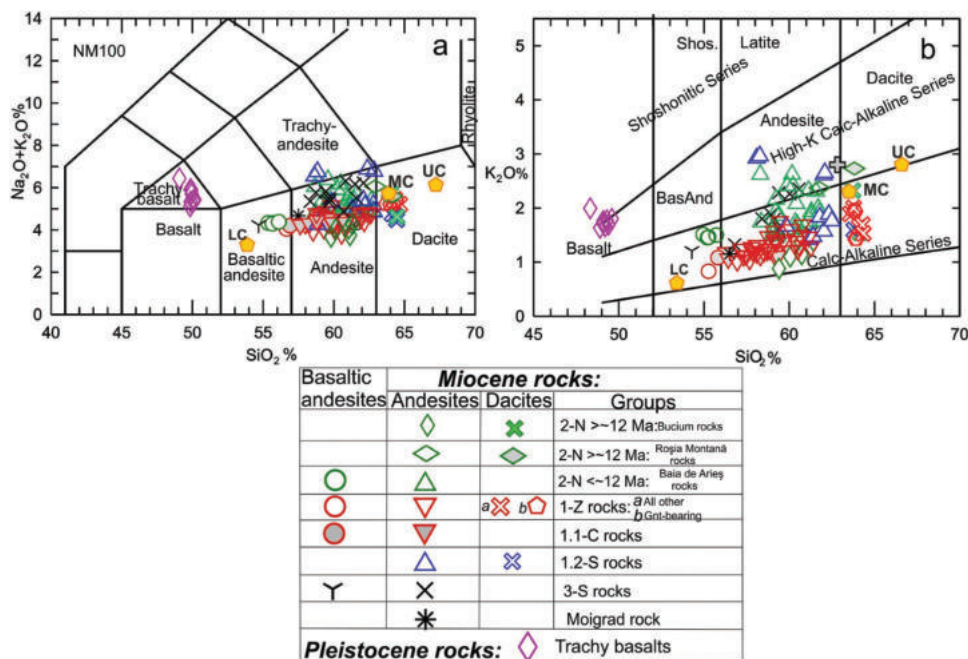

Figure 3. A) Total alkali vs. Silica (TAS) diagram (Le Bas et al. 1986) and b) K_2O vs. SiO_2 (Peccerillo and Taylor 1976) for Apuseni Mts. rocks and the symbols corresponding to the separate basins and age for the Group 2-N (green symbols); All the data are included in the Supplemental table S2.2; LC-Lower crust; MC- Middle crust; UC-Upper crust (after Rudnick and Gao 2003).
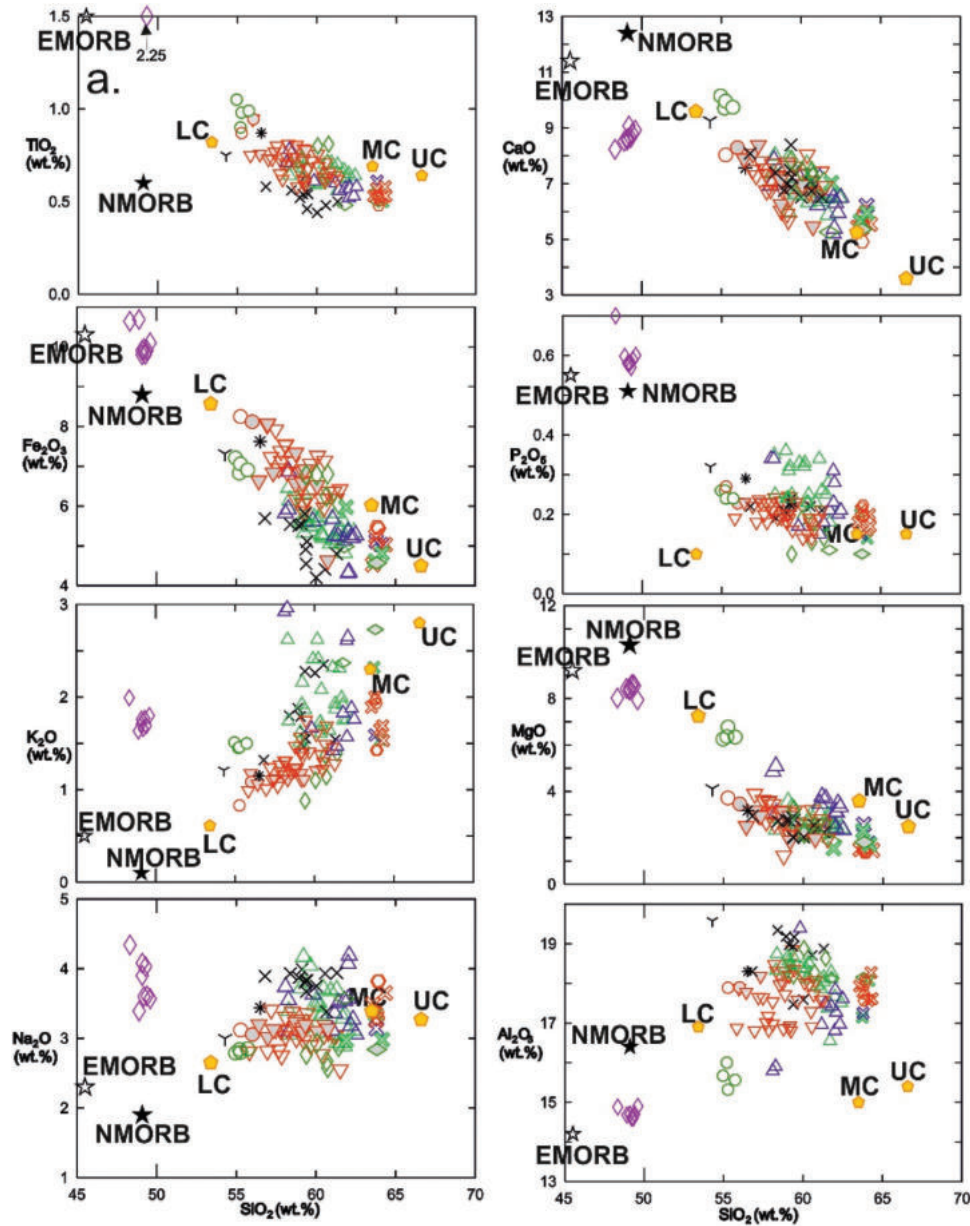
Figure 4. *A) Major and b) trace elements Harker-type variation diagrams for the Apuseni Mts. rocks. Symbols as in* Figure 3; *LC-Lower crust; MC- Middle crust and UC-Upper crust after* Rudnick and Gao (2003); *NMORB and EMORB after* Sun and McDonough (1989)

estimates of upper, middle, and lower continental crust compositions (Rudnick and Gao 2003).

The trace-element trends differ from the major elements in showing enhanced separation between rocks from the different basins. Lanthanum, Ba, Sr (Figure 4b) and Pb (Supplemental online figures S3.1) are variably enriched in rocks from Groups 1.2-S, 2-N (<12 Ma), and 3-S. These rocks are also variably depleted in high-field-strength elements (HFSE) such as Nb. Zirconium in Figure 4b does not follow any particular trend. However, the Zr values for Groups 1.2-S, 2-N (<12 Ma), 3-S, and also for the garnet-bearing dacites (Group 1-Z), are low compared to rocks with similar SiO_2 from Groups

1-Z and 1.1-C. As for the major elements, the trace-element range of the Group 1-Z rocks mostly plot between the lower and upper crustal average estimates of Rudnick and Gao (2003). Rubidium shows a similar trend for all the Miocene Apuseni Mts. rocks with increasing SiO_2. Concentrations of Sc, V, and Co (Figure 4b; Supplemental Figure 3.1) generally decrease with increasing SiO_2. Cr is highest for the Detunata basaltic andesites (Group 2-N; <12 Ma; >200 ppm) and is also relatively high for some Group 1.1-C andesites, Groups 1.2-S and 2-N rocks.

In the CI chondrite-normalized rare-earth element (REE) diagrams (Figure 5), rocks in Groups 1-Z, 1.1-C,

and 2-N > 12 Ma show similar patterns. They show moderate light rare earth element enrichment (LREE), and a flatter slope for the middle (MREE) and heavy rare earth element (HREE) patterns, similar to the pattern of the Lower-Middle crust ((La/Sm)$_N$ = 1.5–3.5; (Dy/Yb)$_N$ = 0.9–1.3, with higher values for garnet-bearing dacites: 1.2–1.5). There is an overall slight or no Eu trough in the REE-patterns of the typical calc-alkaline rocks >12 Ma (Eu/Eu* = 0.8–1.0). The patterns for rocks in Groups 1.2-S, 2-N (<12 Ma), and 3-S are richer in LREE and show similar flat and uniform MREE and HREE patterns, the highest for a few Group 1.2-S andesites and Group 3-S rocks, much higher than the Lower Crust (most rocks show (La/Sm)$_N$ = 3–7 with higher values for Group 3-S rocks = 5–9 and a few Group 1.2-S andesites = 6.2–7.2; high (Dy/Yb)$_N$ = 0.8–1.4 for Group 3-S rocks and 1.2–1.6 for a few Group 1.2-S andesites). There are no obvious Eu anomalies in these areas; they are sometimes slightly positive for rocks of Group 2-N < 12 Ma (Eu/Eu* = 0.9–1.15).

The primitive mantle-normalized (Sun and McDonough 1989) multielement diagrams for the Miocene Apuseni Mts. magmatic rocks show similar patterns to those of typical calc-alkaline arc volcanic rocks from subduction-related tectonic settings (e.g. GEOROC database; e.g. Andes), but are also not very different from the lower continental crust (Figure 6). They are characterized by various enrichments in LILE, U, Th, and Pb, and to a lesser extent in LREE relative to the HREE and HFSE (La/Nb = 1–4). Marked troughs are evident for Nb, Ta, and Ti, and sometimes P and Zr. Overall, the rocks >12 Ma (Group 2-N and 1-Z rocks) display similar trace-element patterns. However, those rocks <12 Ma from Groups 1.2-S, 2-N, and 3-S show extreme enrichments in LILE, with less enrichment in Rb, Pb, U, and Th.

6.2 Isotopes

There is wide variation in Sr isotopic ratios, while Nd isotopic ratios are less variable (Figure 7a). The high-Sr/Y rocks from Groups 1.2-S, 2-N (<12 Ma), and 3-S have lower $^{87}Sr/^{86}Sr$ and higher $^{143}Nd/^{144}Nd$ ratios, on the mantle side of the Bulk Silicate Earth reservoir (Zindler and Hart 1986), compared to the typical calc-alkaline rocks of Groups 1-Z, 1.1-C, and 2-N (>12 Ma), which are much more scattered. Basaltic andesites <12 Ma from Groups 1-Z and 1.1-C also show lower $^{87}Sr/^{86}Sr$ and higher $^{143}Nd/^{144}Nd$ ratios (Figure 7a). The $^{206}Pb/^{204}Pb$ vs. Sr isotopic ratio plots show distinctions between the typical calc-alkaline and high-Sr/Y rocks with the aforementioned two exceptions (Figure 7b), with the typical calc-alkaline rocks trending to EMII. Typical calc-alkaline rocks show high $^{208}Pb/^{204}Pb$ (38.6–38.8) and

$^{207}Pb/^{204}Pb$ (15.65–15.67), moderate to high $^{87}Sr/^{86}Sr$ (0.7047–0.7085) and low (5.5‰) to high δ O$_{wr}$ (>7‰) values. On the other hand, the high Sr/Y rocks show low $^{87}Sr/^{86}Sr$ (0.7040–0.7045), low $^{208}Pb/^{204}Pb$ (38.2–38.6) and $^{207}Pb/^{204}Pb$ (15.59–15.63) and low δ $^{18}O_{wr}$ (5.5–5.7‰) (Roşu et al. 2004; Seghedi et al. 2004; Harris et al. 2013).

The δ^{18}O values of mineral separates and groundmasses obtained for three typical calc-alkaline and four high-Sr/Y samples (Seghedi et al. 2007) are in the range 5.5–5.6‰ for all clinopyroxenes and one amphibole and biotite; these are very close to mantle values (Figure 7c). The δ^{18}O values of the plagioclase and groundmass are higher (7.2–10.1‰), but vary in different areas. The δ^{18}O values of clinopyroxene and amphibole from Groups 1.2-S and 2-N (<12 Ma and high-Sr/Y rocks) and Group 1-Z (typical calc-alkaline rocks) show values that are similar to those for primitive mantle clinopyroxene range (Figure 7c). One sample from Group 2-N (>12 Ma) shows a shift to higher $^{87}Sr/^{86}Sr$ ratio. There is a weak positive correlation between Sr-isotopic ratios and δ^{18}O of minerals and groundmass during crystallization, consistent with increasing degree of differentiation, which is more pronounced for the typical calc-alkaline rocks. In two samples, the $^{87}Sr/^{86}Sr$ ratio of the groundmass is lower than that of the plagioclase.

The whole rock δ^{18}O variations vs $^{87}Sr/^{86}Sr$ useful to identify and quantify distinction between source contamination and crustal assimilation (Figure 7d; simplified after Seghedi et al. 2004 with new data) show that most of the Groups 1Z, 1.1-C, and 2 N < 12 Ma, with exception of a dacite of the Group 1-Z that has a higher δ^{18}O and a slightly higher $^{87}Sr/^{86}Sr$ values (sample 401) are among the most primitive isotopically in all Carpathian – Pannonian Region, with exception of some minor rocks in the East Carpathians (Mason et al. 1996; Figure 7d). The high $^{87}Sr/^{86}Sr$ and δ^{18}O of an andesite belonging to the Group 2-N > 12 Ma (alike as in Figure 7c; sample 790) show a trend towards source contamination. In contrast, the Western, Central, and Eastern Carpathian volcanic rocks, with exception of the South Harghita (SH), show different trends that prove significant crustal implication for those magmas (AFC processes), as well as the implication of source contamination (Seghedi et al. 2004).

7. Discussion

7.1 Magma differentiation processes

The effects of differentiation processes such as assimilation, fractionation, and magma mixing in the Apuseni Mts. were previously discussed in the context of the
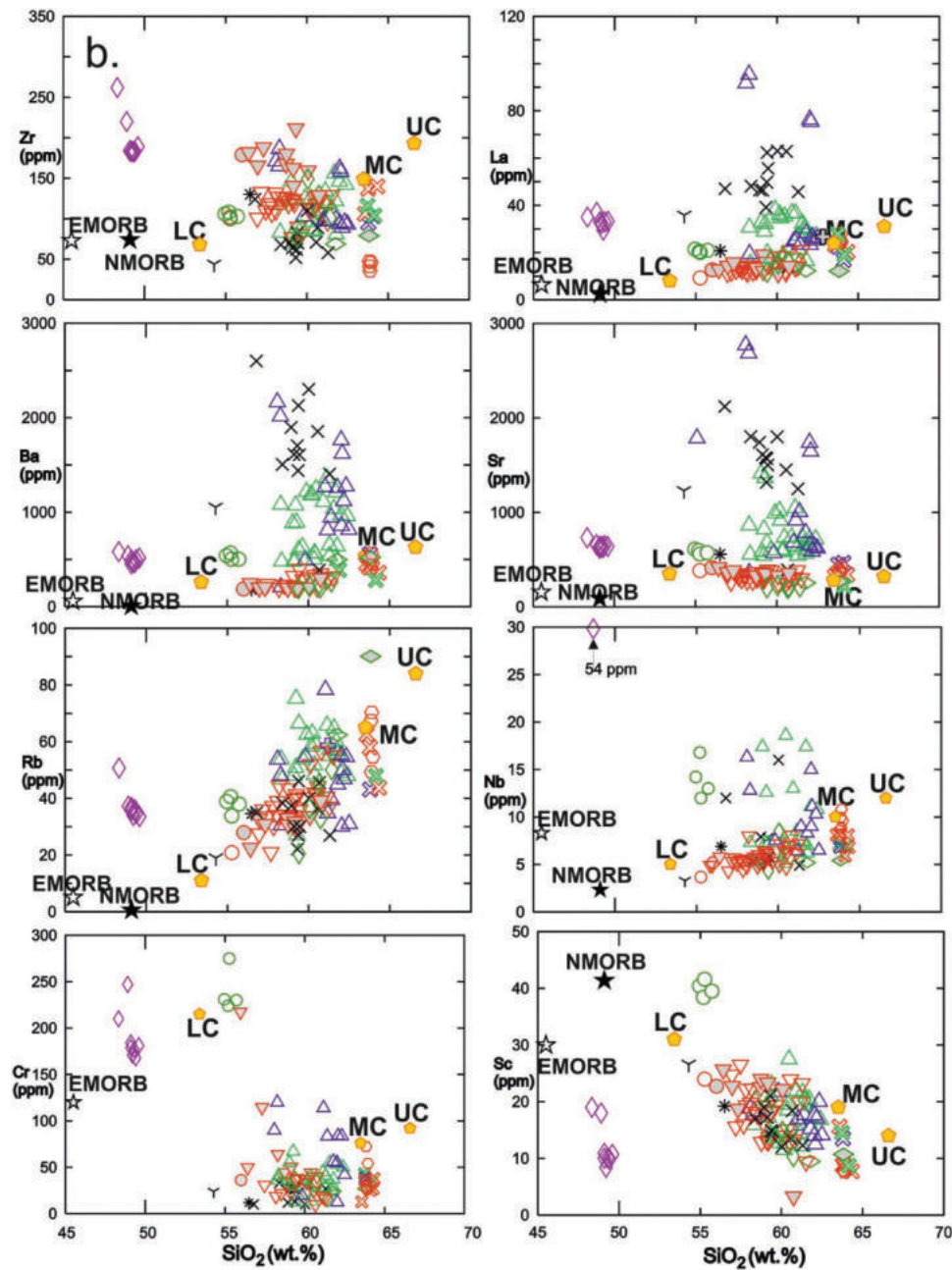
Figure 4. Continued.

much larger Carpathian-Pannonian region (Seghedi *et al.* 2004). Some of these processes can be deduced from petrological evidence. Most Apuseni igneous rocks are phenocryst-rich (~55–70%), dominated by plagioclase, and show a decrease in modal abundances of clinopyroxene and orthopyroxene towards the more evolved rocks, while amphibole, biotite (mostly in high-Sr/Y rocks), and plagioclase increase in abundance. Mafic minerals are mainly unzoned, whereas plagioclase mostly shows normal zoning. However, there are many examples of plagioclase and/or amphibole phenocrysts displaying disequilibrium features such as resorbed shapes, oxidation, or sieve textures, which suggest that the whole-rock geochemical composition was controlled by fractional crystallization ± assimilation (Figure 7a), but also by magma mixing. The rocks showing plagioclase resorption suggest disequilibrium. Such textures indicate rapid changes in the thermo-chemical characteristics of the magmatic system, driven by magma mixing (e.g. Bontău volcano and Caraci volcano where the last eruptions were basaltic andesite; Supplemental figure S3.3). According to Harris *et al.* (2013), opacitic rims of amphibole phenocrysts in rocks from Deva-3 area show evidence for two episodes of mixing; the same authors
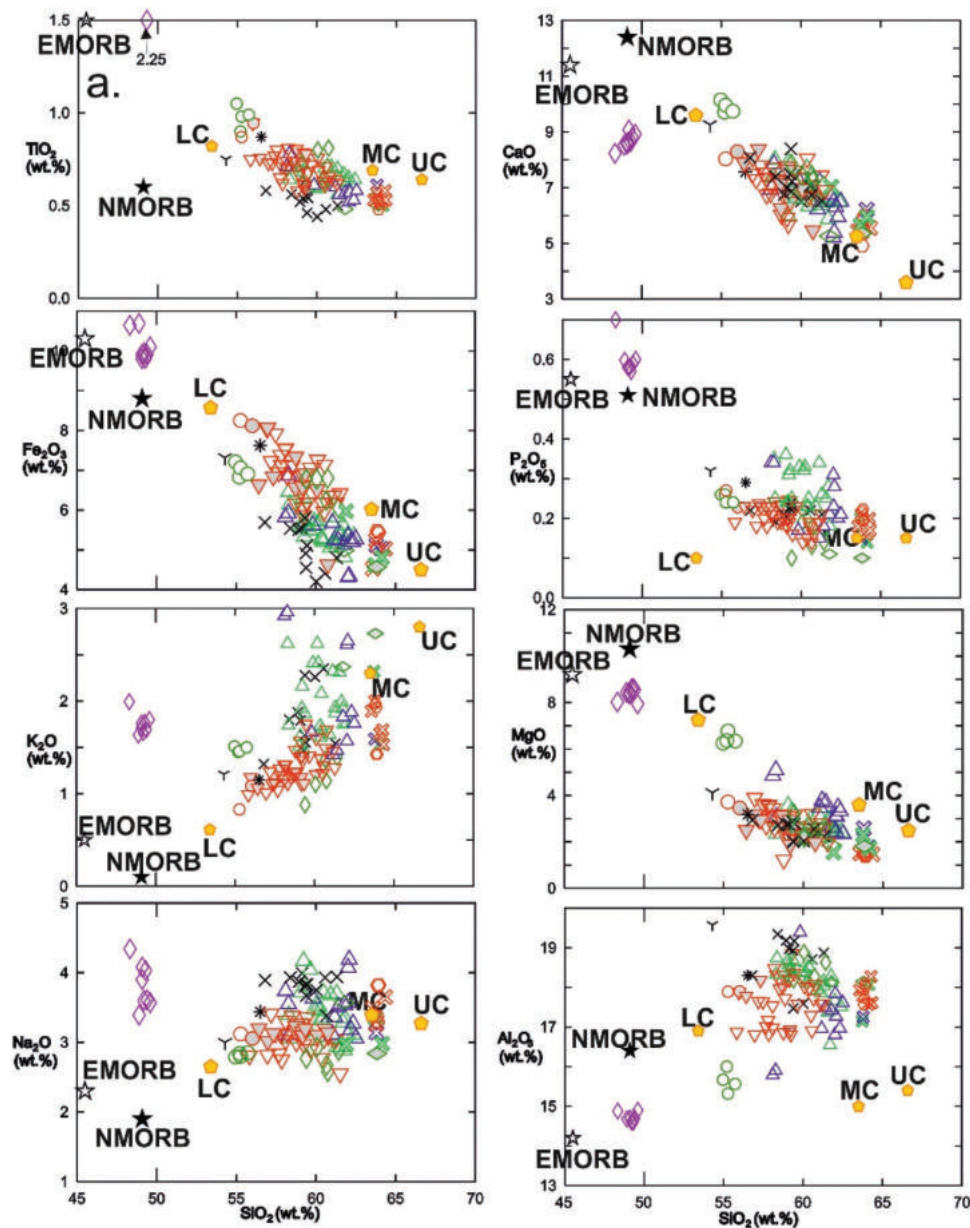
Figure 4. *A) Major and b) trace elements Harker-type variation diagrams for the Apuseni Mts. rocks. Symbols as in* Figure 3; *LC-Lower crust; MC- Middle crust and UC-Upper crust after* Rudnick and Gao (2003); *NMORB and EMORB after* Sun and McDonough (1989)

also highlight the presence of enclave and magma mingling textures in the Barza magmatic centre (Group 1-Z). In Figure 7c, two samples have lower $^{87}Sr/^{86}Sr$ ratios in the groundmass than in the plagioclase, which may also signify mixing with new magma batches (e.g. Tepley *et al*. 2000).

Major-element variation diagrams of the examined rocks (Figure 4a) show poorly defined trends from basaltic andesites to dacites. Al_2O_3 shows a very poor trend with increasing SiO_2. With the exception of Rb, which is displaying a positive correlation (Figure 4b), trace elements also show very weak trends but strongly enriched values for La, Ba, Sr, Pb, and Th, especially for rocks

<12 Ma in Groups 1.2-S, 2-N, and 3-S. These rocks were collectively defined as high-Sr/Y rocks (e.g. Roşu et al. 2004, Harris *et al*. 2013) and have been considered 'adakite-like' (rocks which show similar geochemical characteristics to adakites without petrogenetic implications).

REE enrichment of typical calc-alkaline and high-Sr/Y rocks of the region (Figures 4, 5 and 6) can be explained by different degrees of fractionation (as most of the rocks formed from evolved magmas), but also by differences in mantle sources, and by different extents of interaction with crustal lithologies. For example, higher LREE and LILE contents are observed in some high-Sr/Y andesites in Group 1.2-S (Figures 5, 6). Some typical
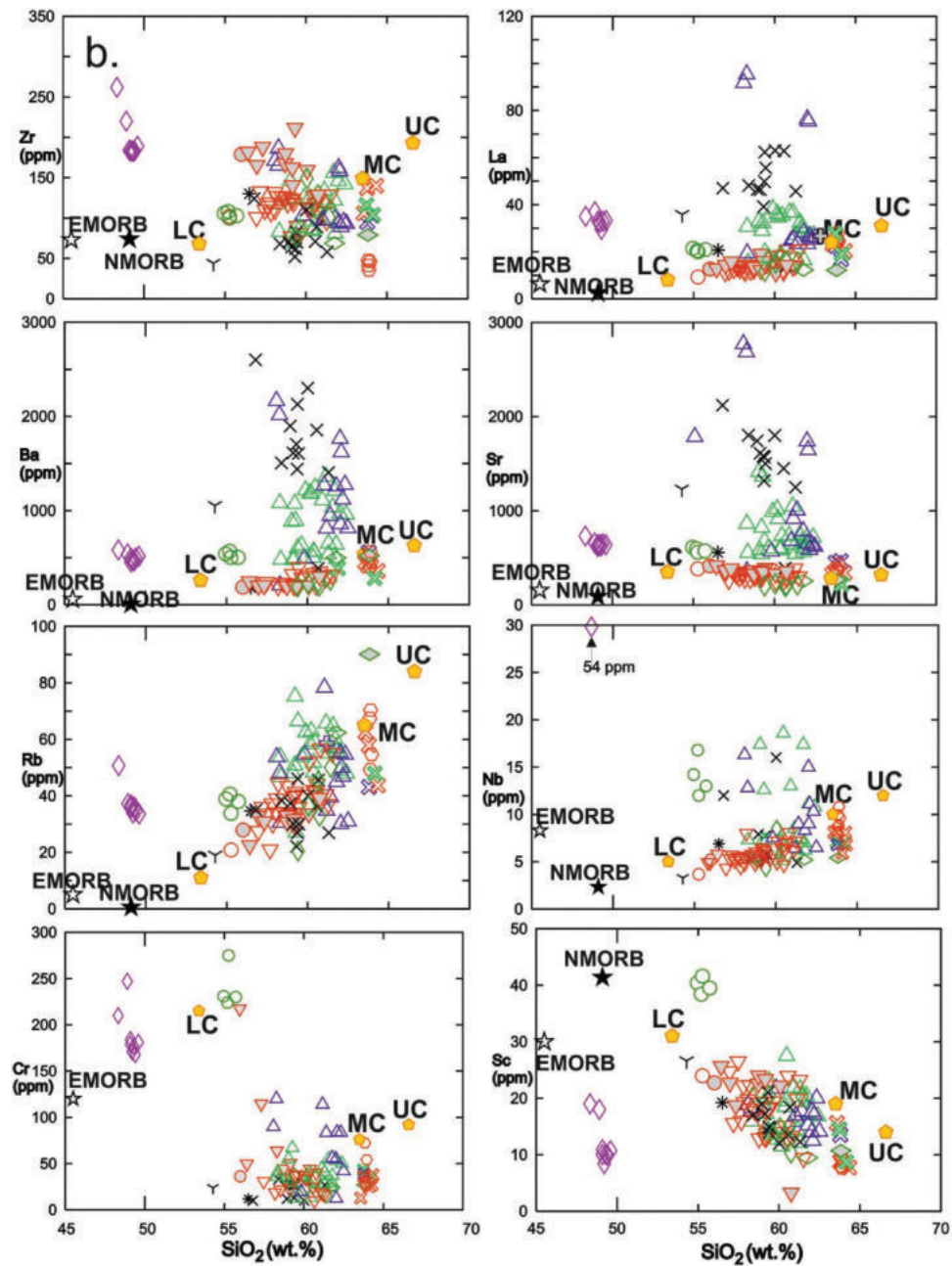
Figure 4. Continued.

andesitic and dacitic calc-alkaline rocks only show a small negative Eu anomaly, suggesting that plagioclase was not the main fractionating phase or that plagioclase was accumulative (as suggested by the high abundance of phenocrysts).

Crustal assimilation is suggested by the increase of $^{87}Sr/^{86}Sr$ and decrease in $^{143}Nd/^{144}Nd$ from basaltic andesites to dacites of Group 1-Z and >12 Ma rocks of Group 2-N (Figure 7a). The high-Sr/Y rocks, which are all <12 Ma, have lower $^{87}Sr/^{86}Sr$ and higher $^{143}Nd/^{144}Nd$ ratios, closer to mantle compositions and were less affected by crustal assimilation and fractionation

(Figure 7d; Seghedi et al. 2004). However, the general increase of $\delta^{18}O$ with respect of mantle values of plagioclase phenocrysts and groundmass, despite showing a narrow range of $^{87}Sr/^{86}Sr$ values, suggests that the magmas <12 Ma (both high-Sr/Y and typical calc-alkaline) experienced crustal assimilation, although much less for the high Sr/Y rocks than for the typical calc-alkaline rocks (Group 1-Z), or those >12 Ma from Group 2-N (Figure 7c). On the other hand, the $\delta^{18}O$ and $^{87}Sr/^{86}Sr$ ratios of early crystallized minerals (clinopyroxenes or amphiboles) in equilibrium with the melt in volcanic rocks <12 Ma are closer to mantle isotopic
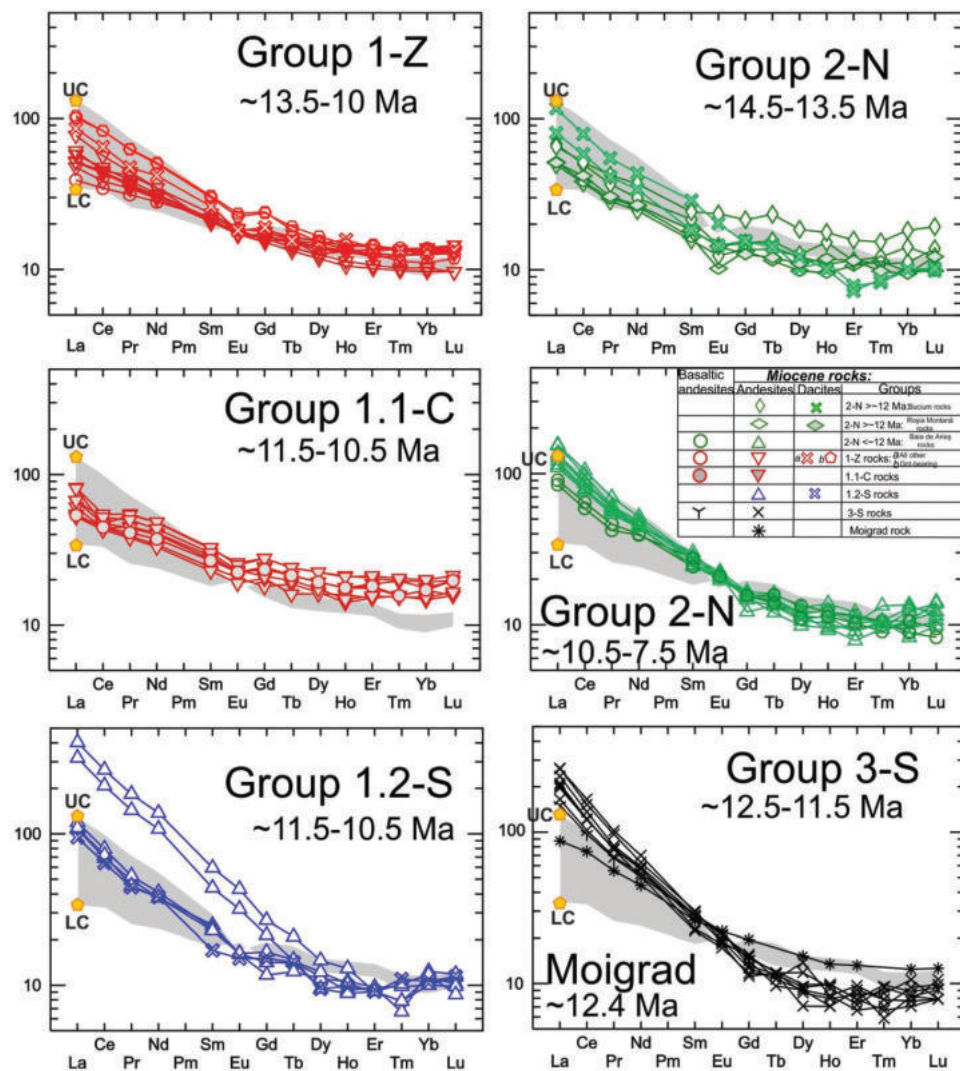
Figure 5. *CI Chondrite-normalized REE diagrams for the Miocene igneous rocks from the Apuseni Mts. Symbols showing in Group 2-N (~10.7–7.5 Ma). LC-Lower crust and UC-Upper crust after .Rudnick and Gao (2003) is shown as shadow. The normalizing values are from Sun and McDonough (1989)*

compositions (Figure 7 c). This suggests that they were generated in a deeper magma chamber and later trapped in a more evolved magma chamber (Seghedi *et al*. 2007). Moreover, the early crystallized minerals (clinopyroxenes or amphiboles) (Figure 7c) fall in the same field of $\delta^{18}O$ and $^{87}Sr/^{86}Sr$ ratios as primitive oceanic arc lavas that represent mantle composition range (e.g. Eiler *et al*. 2000).

Negative Nb and Ta anomalies in primitive mantle-normalized diagrams (Figure 6) could be either the result of a mantle source affected by subduction-related components, as interpreted by Roşu *et al*. (2004) and Harris *et al*. (2013), or lower crustal melting (with similar Nb and Ta troughs) or mixing of melts from these two sources. However, since primitive rocks are absent, a bulk mixing model using whole-rock $\delta^{18}O$ vs. $^{87}Sr/^{86}Sr$ data, between a magma derived from a depleted mantle source and

average local sediments, already suggested for all the rocks <12 Ma, implies that a mantle source affected by subduction components is less significant (Figure 7d; Seghedi *et al*. 2004). An exception is the typical calc-alkaline rocks of Group 2-N > 12 Ma; these rocks display a shift to higher $^{87}Sr/^{86}Sr$ and $\delta^{18}O$ ratios that may suggest either that their source was mantle affected by subduction-components or the source was continental lower crust (Figure 7c, d).

The 'adakite-like' rocks (Roşu *et al*. 2004; Harris *et al*. 2013), here our 'high-Sr/Y group' are not always source-dependent. Crustal assimilation and crystal fractionation involving amphibole and clinopyroxene for some adakite-like rocks are not necessarily connected to source processes (e.g. Richards and Kerrich 2007). Amphibole and clinopyroxene fractionation are suggested by the Dy/Dy* (0.4–0.8) versus Dy/Yb (1.2–2.2) (Davidson *et al*. 2013;
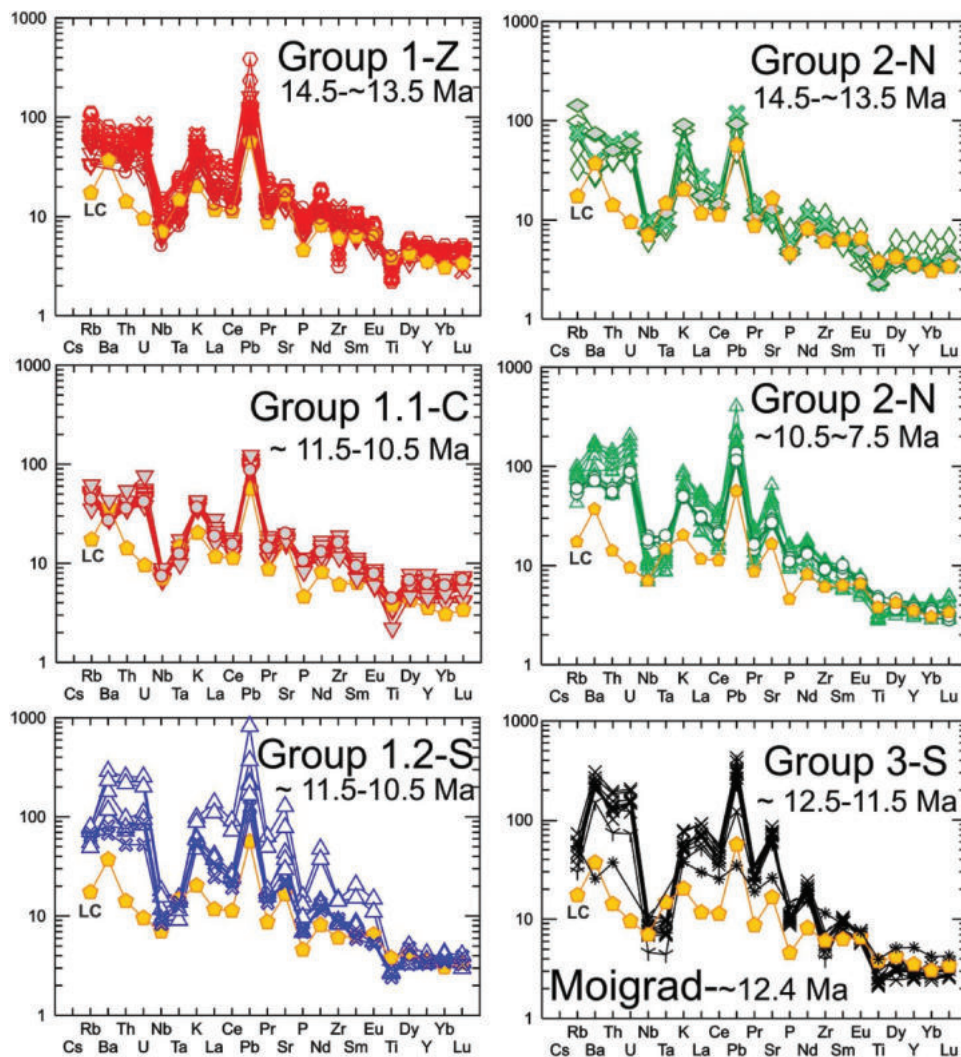
Figure 6. *Primitive mantle-normalized multielement diagrams for the Miocene igneous rocks from the Apuseni Mts. (symbols as in* Figures 3 *and* 5*). LC is lower crust after* Rudnick and Gao (2003). *The normalizing values are from* Sun and McDonough (1989)

Supplemental online figure S3.2) for all the Apuseni rocks, and particularly for the high Sr/Y samples by showing slightly lower Dy/Dy* (0.4–0.6) with respect to Dy/Yb for high-Sr/Y rocks.

7.2 Time-related spatial geochemical variation

In Figure 8, which shows Sr/Y ratios as a function of ages (Ma), the main Group 1-Z magmas evolved over the longest period of activity (~4 Myrs) and display low Sr/Y ratios and typical calc-alkaline compositions. With the exception of Group 1.1-C, in which the magmas have normal calc-alkaline compositions, magmatism in all the other, smaller basins evolved over much shorter time periods, <1-1.5 Myrs, for Group 2-N with variably high Sr/Y ratios, and Group 1.1-C. Magmas erupted in each sub-basin show a large variation in Sr/Y (>50) as well as

Ba with the highest Sr/Y mostly in smaller rock volumes (e.g. dykes or small intrusions; Roşu *et al.* 2004). The K/Ar age data indicate that the tectonic sub-basin development started with the Group 3-S, after 12 Ma followed by Groups 1.2-S and 2-N, through contamination processes that developed mainly in the Jurassic ophiolite units (Figure 1b; Nicolae and Saccani 2003; Bortolotti *et al.* 2002; Gallhofer 2015).

The episodic, low-volume magmatism in Group 2-N covered the entire time interval of magma evolution in the Apuseni Mts. (14.5–7 Ma). In addition, the youngest products in Group 2-N, the Detunata basaltic andesites (7.2–8 Ma), are the least evolved in the region. These are different from the other basaltic andesites from the area (which have 14–22 ppm Ni and 24–36 ppm Cr), in having the highest Ni (26–54 ppm) and Cr (224–275 ppm) and higher La/Yb (10–14), similar to the local Pleistocene Na-alkali basalts (14–17) (Downes *et al.*
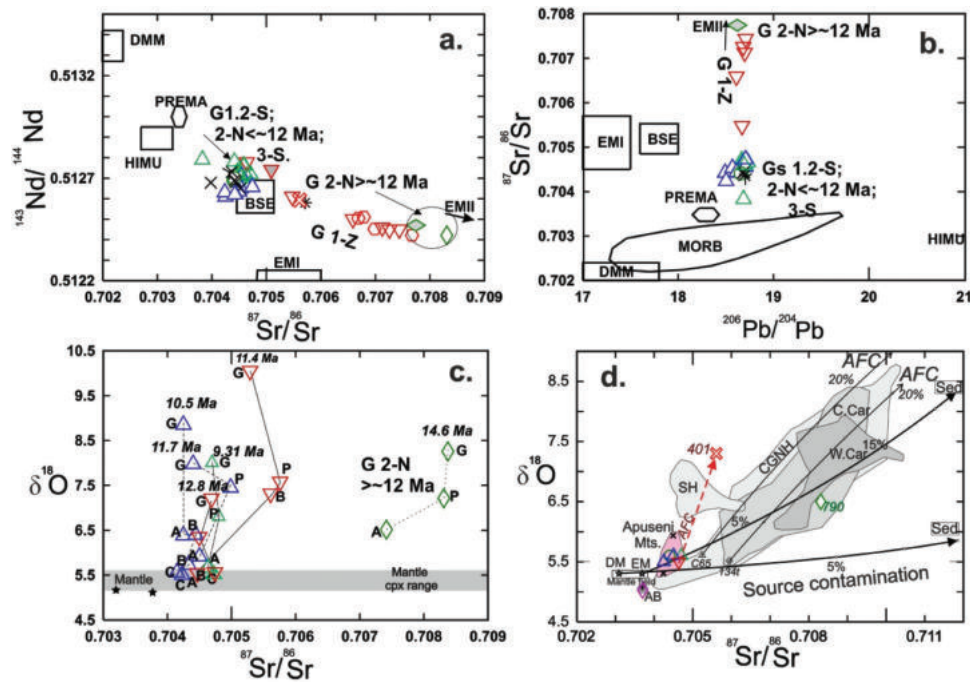
Figure 7. A. $^{87}Sr/^{86}Sr$ vs. $^{143}Nd/^{144}Nd$ ratios b. $^{206}Pb/^{204}Pb$ vs. $^{87}Sr/^{86}Sr$ vs.; c. $\delta^{18}O$ mineral vs. $^{87}Sr/^{86}Sr$ mineral diagrams for the Miocene Apuseni Mts. rocks after (Seghedi et al. 2007); d. $\delta^{18}O$ whole rock vs. $^{87}Sr/^{86}Sr$ whole rock for the Carpathian-Pannonian region after (Seghedi et al. 2004); abbreviations: C-clinopyroxene; A-amphibole; B-biotite; P-plagioclase; G-groundmass and the lines link data from the same sample; Sed-average local sediments; W.Car- Western Carpathians rocks; C.Car- Central Carpathians rocks,; CGNH- Călimani-Gurghiu -North Harghita rocks; SH – South Harghita rocks; Mantle $\delta^{18}O$ and $^{87}Sr/^{86}Sr$ minerals according to Eiler et al. (2000;. DMM, MORB, PREMA, HIMU, BSE, EMI, EMII after Zindler and Hart (1986). Symbols as in Figures 3 and 5. Modelling of assimilation fractional crystallization (AFC) and bulk mixing models with average local sediments (Sed) – for Carpathian – Pannonian volcanic rocks in fig d are using parameters given in the Figure 8 of (Seghedi et al. 2004).

1995; Tschegg et al. 2010). One tentative hypothesis to be investigated in the future is that the Group 2-N magmas responded to sudden short-term tectonic changes. At a regional scale, the main period of magmatic evolution dominated by rocks with high Sr/Y ratio was coeval (~12–10 Ma) with shortening in the East Carpathians (Mațenco and Bertotti 2000), but also with the extension in the main Pannonian Basin (Mațenco et al. 2010; Merten et al. 2011; Balázs et al. 2017; Van Hinsbergen et al. 2020).

The ~12–10 Ma garnet-bearing dacites in Group 1-Z suggest that the regional stress field was extensional during this time, because garnet is not stable at shallow depths and its preservation therefore requires rapid ascent of the host magma to the surface (e.g. Harangi. et al. 2001; Harangi. and Lenkey 2007; Bach et al. 2012). Similar rocks have been described by Harangi. et al. (2001) elsewhere in the Carpathian region and suggest partial melting of a garnet-bearing (eclogitic) lower crust. The low Hf/Sm ratios coupled with Zr/HREE and Hf/HREE fractionation in garnet-bearing dacite point to the involvement of eclogitic rocks in the source (Van Westrenen et al. 2001).

7.3 Continental crust and/or subcontinental mantle contribution for the source of the Apuseni Mts. Miocene magmas

7.3.1 Depleted vs. enriched mantle components

We use ratio as Zr/Nb and Y/Nb to distinguish between depleted mantle (MORB-source) versus an enriched intraplate component (OIB-source) in the Apuseni Mts. magmas (e.g. Jicha et al. 2009; Figure 9).

There is a large range in Zr/Nb ratios (6.2–37.8) that generally vary along a line with decreasing Y/Nb from basaltic andesites of Group 1-Z to the basaltic andesites of Group 2-N (Detunata) (Figure 9). A shift of higher Zr/Nb is characteristic for the Group 1.1-C (Caraci). This array may represent either mixing between magmas derived from enriched source similar with that of the intraplate basalts and more depleted mantle sources or it may represent a variation of partial melting of a similar dominantly enriched source. The group 3-S merely covers the local sediments; the Roşia Montană andesite-dacite has similar values with average Lower continental crust and the garnet-bearing dacites show the lowest Zr/Nb ratio.
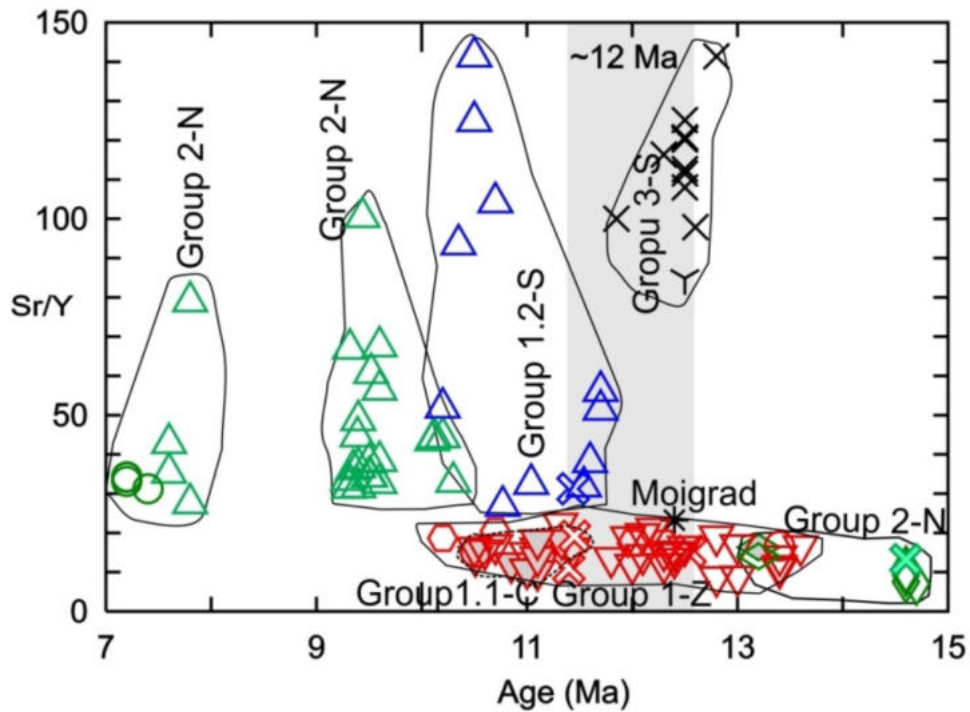
Figure 8. *Sr/Y vs. age (Ma) for the Miocene magmatic rocks from the South Apuseni Mts. The shaded area shows the maximum time boundary between typical calc-alkaline and high Sr/Y calc-alkaline rocks according to K/Ar dating (new and literature data). Symbols as in Figure 3.*

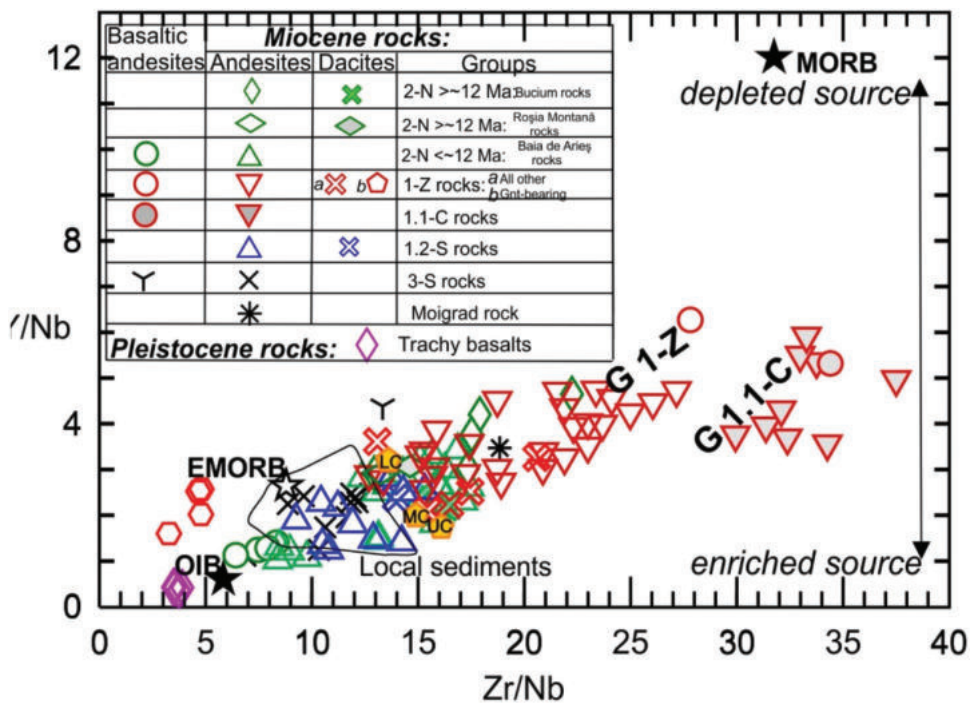**Figure 9.** *Zr/Nb vs. Y/Nb for the Apuseni Mts magmatic rocks. Local sediments are shown after .Mason et al. (1996). LC-Lower crust; MC-Middle crust and UC-Upper crust after Rudnick and Gao (2003); NMORB and EMORB after Sun and McDonough (1989)*

7.3.2 Melt generation depth challenge

According to global compilations, the geochemistry of arc and continental magmatism is sensitive to Moho depth (e.g. Chapman *et al.* 2015; Profeta *et al.* 2015; Hu *et al.* 2017). These articles all use Sr/Y as a common qualitative indicator of the average crustal depth at which level magmatic differentiation occurred. The results suggest that rocks with higher Sr/Y ratio signify a greater pressure or depth (e.g. Chapman *et al.* 2015). As we have discussed already for the Apuseni Mts. the rocks from various graben systems show a high and variable Sr/Y ratio, specifically after 12 Ma (Figure 8). We may deduce that variable Sr/Y ratio could be connected with different crustal thicknesses where the magmas were produced at the base of the crust. Although our compilation of data for Apuseni Mts. is not sufficiently representative to apply empirical formulas for crustal thickness for individual Groups (e.g. Profeta *et al.* 2015; Hu *et al.* 2017).

As Sr content shows a very large variation in the Apuseni Mts., and assuming that Sr is an indicator of depth it looks like a primary feature that may characterize the source region of the magmas (e.g. higher Sr in rocks indicate magmas extracted at pressures >12 kbar and enters in the liquid phase where it is incompatible and where plagioclase is unstable; Petford and Atherton 1996), we discuss plots of Sr vs. Age and vs. SiO_2 (Figure 10 a, b). Concentrations of Sr (also Y, La, Yb, Nb, and Ta) in the melt may also reflect the enrichment of this element in the source (e.g. Kendrick and Yakymchuk 2020).

We also discuss plots of Rb/Sr ratio vs. age and vs. SiO_2 (Figure 10 c, d) since Sr and Rb contents generally increase with differentiation until the onset of significant plagioclase feldspar fractionation when Sr decreases (e.g. Davidson 1998). Since Rb does not decrease during differentiation, increased Rb/Sr is an indicator of fractionated magmas. In this situation, even if we cannot deliver real estimates for crustal thickness, we can appreciate the relative variances between the different groups.

In Figure 10, a, b, the Group 2-N rocks (>12 Ma) have lower Sr contents (~200 ppm), whereas samples of Groups 1-Z and 1.1-C are slightly higher (300–400 ppm), and most rocks of Groups 1.2-S and 2-N (<12 Ma) have much higher (~600 ppm) and similar Sr contents, regardless of SiO_2 variation. The highest Sr content (starting at 1250 ppm up to 2000 ppm) belongs to Group 3-S rocks. This suggests that, since there is a characteristic Sr content for the mentioned groups, there was an increase in crustal thickness for melt generation of Group 2-N (>12 Ma) up to Group 3-S rocks. This correlates with the tectonic situation that suggests a thinner crust below the main Zărand graben basin (28–32 km) and a progressively thicker crust towards the Săcărâmb, Roşia Montana – Baia de Arieş areas (32–
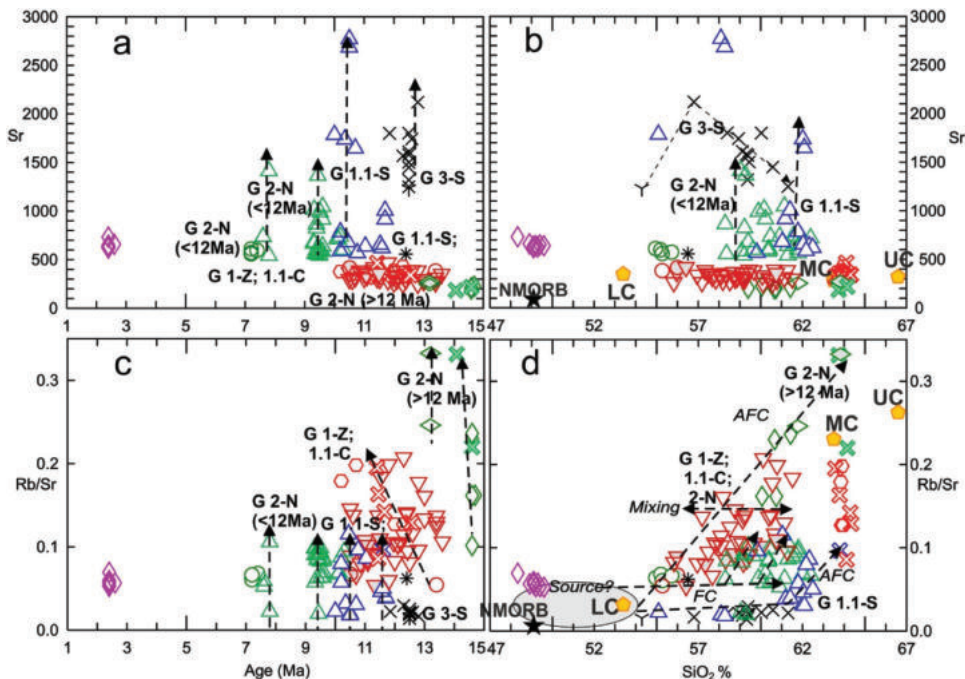

Figure 10. A, b, c, d. Sr and Rb/Sr ratio vs. Age (Ma) and SiO_2 for the Miocene magmatic rocks in Apuseni Mts., including Pleistocene trachybasalts. LC-Lower crust; MC-Middle crust; UC-Upper crust after .Rudnick and Gao (2003); NMORB (black star) after Sun and McDonough (1989). *Symbols as in the* figures 3 *and* 9

35 km) and the thickest for the Deva area (~35 km) (Bala et al. 2017). The anomalous high-Sr trends of Group 2-N (<12 Ma) and Group 3-S (with smallest volume of extruded rocks) need a different explanation that may infer crustal contamination and/or larger volume of crustal melts (see further discussion).

Figure 10 a, b shows that most important fractionation trend (from basaltic andesites to dacites) is found in Group 1-Z, in the main area of magmatism. The high-Sr Groups suggest only short differentiation trends (FC/AFC) over different time intervals. The most primitive and youngest Detunata basaltic andesite has Sr content in the same range with Group 2-N (<12 Ma), but also similar to Pleistocene alkali basalts suggesting a similar source. As Sr content decreased in differentiated magmas, dacites from all groups mostly do not plot on the trend of the evolved andesites, as Sr was fractionated in plagioclase. The high Rb/Sr of the Group 2-N (>12 Ma) dacites (Figure 10 c, d) may suggest crustal involvement (either as mixing between mantle and crustal sources or as crustal contamination). The variation of SiO_2 for the same Rb/Sr ratio suggests magma mixing, as perceived in petrography (e.g. Groups 1-Z; Figure 10 d). Also in Figure 10, we suggest the possible sources for Apuseni Mts rocks as various enriched mantle and/or lower crust (see further discussion).

Group 3-S (Deva area) has the most unusual behaviour, showing the highest Sr that decreases with increasing SiO_2 (possibly related to plagioclase fractionation of the melts), as well lowest Ta values similar with Lower crust values (Supplemental figures S3.1). Also Group 3-S has the lowest Rb/Sr for all the rocks showing a low range of Rb content with increasing SiO_2 (from 20 to 40 ppm) as compared with all the other groups that have 70–80 ppm Rb for the evolved rocks. This unusual composition may rather suggest a lower crustal origin via partial melting of amphibole-rich lower crust (e.g. Davidson et al. 2007) rather than mantle melting.

Zr and Hf that are considered to behave nearly identically during magmatic processes (e.g. Hoskin and Schaltegger 2003) show similar values for the basaltic andesites in the Apuseni Mts. ranging close to NMORB-EMORB and lower continental crust (LC) compositions (Zr/Hf ~36.3). All the andesites and dacites have Zr/Hf = 30–42, with the exception of the garnet-bearing dacites, which show the lowest Zr/Hf (22–25).

7.3.3 The lesson of large ion lithophile elements (LILE)

In Figure 11, it is difficult to explain the elevated concentrations of large ion lithophile elements (LILE), such as Ba and Sr in some Apuseni Mts. rocks. In the $^{87}Sr/^{86}Sr$ vs. Sr diagram (Figure 11a), AFC processes are suggested

for Groups 1-Z, 1.1-C, and 2-N (>12 Ma), and fractional crystallization for Groups 2-N (<12 Ma) and 1.2-S. The increased Sr in a few rocks in these groups may suggest local crustal contamination rather than source contamination. Group 3-S rocks may be interpreted via a partial melting scenario of a high-Sr amphibole-rich lower crust, as well as a composite source of mantle and lower crust melts (see further discussion).

The high Ba/Nb ratio of the high-Sr/Y rocks may not be associated with conventional 'slab-derived fluid' (high Ba/Nb of samples from Groups 1.2-S and 2-N; Figure 11 b) or high La/Zr ratio with conventional 'sediment-derived melt' (high La/Zr of few Group 1.1-C rocks and all samples of Group 3-S = 0.45–0.9) signatures (e.g. Hawkesworth et al. 1993) of the local mantle. Rather, they point to magma fractional crystallization in a 'hydrous' (i.e. dominant amphibole ± biotite lithologies) crustal environment that caused contamination with high LILE, LREE, and Th. In addition, according to Seghedi et al. (2004), Seghedi et al. (2007)), the correlated variations of Sr and O isotopes with increasing SiO_2 indicate that most of the Apuseni Mts. magmas were formed via minor crustal contamination combined with fractional crystallization (Figure 7). This may suggest that the Sr, Nd, and O isotopic composition of the contaminant for the high-Sr/Y magmas was closer to that of the mantle source, but the composition was very rich in LILE. This LILE-enrichment may be explained by the fact that most of the samples from the Miocene sub-basins that show high LILE values are <12 Ma and lie within the largest Middle Jurassic ophiolitic accretionary sequence of the Carpathians (e.g. Bortolotti et al. 2002) and less in adjacent Mesozoic accretionary metamorphic terranes (Figure 1b), displaying an isotopic composition of MORB-source mantle (Gallhofer et al. 2017). Assimilation of mafic ophiolite crust would have a minimal effect on the isotopic composition of Sr, Nd, and Pb, making difficult to detect this component in a contamination scenario. A LILE-rich contaminant associated with ophiolite rocks is difficult to recognize, but their association with silica-poor limestones/dolomitic layers and possible skarn formations provides a viable explanation for the variably strong Sr anomaly in the high-Sr/Y groups (e.g. Wenzel et al. 2001). Also, this may explain the large compositional contrasts between neighbouring volcanoes and closely associated basins, and their similar time of emplacement (e.g. Group 2-N in Figure 2). Plots of SiO_2 vs. LILE and HFSE (Figure 4b) rather reflect local variability of the crustal contribution and less of the metasomatized mantle (e.g. Hildreth and Moorbath 1988).

In contrast, rocks from the same time period as the high-Sr/Y rocks (<12 Ma) that developed as Groups 1.1-C and 1-Z exhibit typical calc-alkaline evolution (AFC and/or mixing). Even though they have been
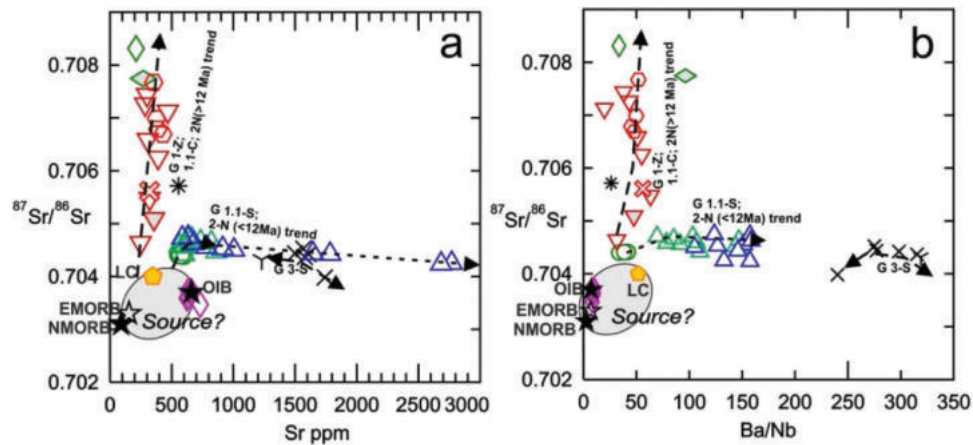
Figure 11. A, b, $^{87}Sr/^{86}Sr$ vs. Sr (ppm) and Ba/Nb diagrams for the Miocene magmatic rocks in Apuseni Mts., including Pleistocene trachybasalts. LC-Lower crust after .Rudnick and Gao (2003); NMORB (black star) and EMORB (white star) after Sun and McDonough (1989). Symbols and data sources as in Figures 3, 5 and 9

generated in a basement dominated by the same ophiolitic sequences, they do not show similar contamination as the high-Sr/Y rocks (Figure 1b). This may suggest that a high-Sr contaminant is missing in the typical calc-alkaline rock of Groups 1.1-C and 1-Z and is not a matter of source contamination in the high-Sr/Y rocks. The highest Ba/Nb belongs to the Group 3-S, reflecting again a source dominated by lower crustal components, probably via partial melting processes.

In order to assess the validity of the potential sources: DMM (depleted mantle), EM (enriched mantle), and LC partial melts in the Apuseni Mts. (same as in Mason *et al.* 1996), we applied assimilation–fractional crystallization (AFC) modelling (DePaolo 1981) using different crustal end-members as contaminants (Figure 12). Using Nb/Y vs. Th/Y modelling (Figure 12a), all the Apuseni rocks, with the exception of those showing an increase in Th (Group 3-S) or deviation to high Nb/Y (Group 2-N < 12 Ma), can largely be explained by AFC of magmas involving all these sources (DMM, EM, or LC partial melts) via assimilation of average local upper crustal compositions (Mason *et al.* 1996).

The diagram of Nb/Y vs. Th/Y is an example of a modelled interaction between magma and crust, in which two magmas, one of depleted composition (derived from DMM) and one of enriched composition (derived from EM), show a shift above the MORB-OIB array by interacting with average LC local crust (Mason *et al.* 1996) using an arbitrary value of r = 0.35 (rate of assimilation vs. rate of crystallization). The relative mass of magma remaining during fusion (F) suggests a decreasing fusion rate starting from the typical to high Sr/Y calc-alkaline magmas in Apuseni Mts. The modelled lower crustal melting may apply only to the high Sr/Y magmas. This figure also may suggest the

probability of a mixed mantle–crustal provenance (MASH zone model; Pearce 2008), with primitive mantle magma causing crustal fusion at the base of the crust and releasing an evolved magma; however, the real local lower crust composition is not known, just estimated from trace element diagrams and required by the modelling.

However, Ba/Rb vs. Rb, $^{87}Sr/^{86}Sr$ vs. Sr and $^{143}Nd/^{144}Nd$ vs. Rb AFC curves are better explained by two-stage processes, the first involving assimilation of average crustal compositions, and the second the assimilation of a high-Sr/Y andesite, assuming that its composition is analogous to the contaminants (Figure 12 b, c), or in the case of Figure 12 d, by variation of 'r' (assimilation rate/crystallization rate) using the local average upper crust as contaminant and suggesting an increased assimilation rate for Groups 1-Z and 1.1-C. As already proposed, this represents a time-dependent development of the magmas, which in case of Group 2-N > 12 Ma may suggest either lower crustal source or assimilation and fractional crystallization (AFC) of normal upper crust, and after ~12 Ma, an enriched upper mantle source for a magma affected less by fractional crystallization but by contamination by a LILE-enriched crust with low isotopic Sr and higher Nd and specific developments at a local scale.

7.4 Geodynamic scenario

Extension-related magma emplacement during the Miocene has been documented in earlier studies (e.g. Roşu *et al.* 2004; Neubauer *et al.* 2005), which suggested that block rotation and asthenospheric upwelling triggered partial melting of the mantle beneath the Apuseni
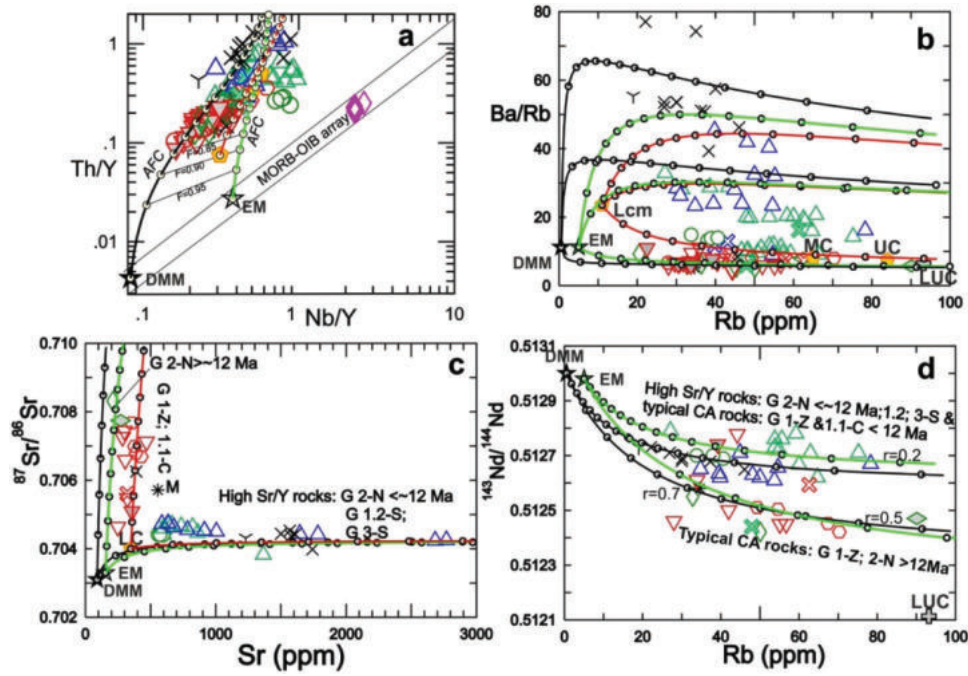
Figure 12. *A) Nb/Y vs. Th/Y, b) Ba/Rb vs. Rb (ppm), c) $^{87}Sr/^{86}Sr$ vs. Sr (ppm) and d) $^{143}Nd/^{144}Nd$ vs. Rb (ppm) diagrams showing results of AFC (assimilation-fractional crystallization) models for the Apuseni Mts. rocks, calculated using Igpet software (.Carr 2010) and (DePaolo 1981) modelling. Upper crustal assimilants include local average upper crust (LUC) after Mason et al. (1998) for typical calc-alkaline rocks and andesites from the Group 3-S (sample 6920), and Group 1.2-S (sample 776) as contaminant for the high-Sr/Y calc-alkaline rocks (Figure 12 b, c). AFC curves are for various combinations of depleted mantle melts (DMM-black lines) and enriched mantle melts (EM-black green lines) and lower crustal melts (LC-red lines). Bulk distribution coefficients (Sr-0.4; Rb-0.04; Ba-0.3; Zr-0.4; Rollinson 1993). Tick marks on curves indicate relative mass of magma remaining (f) in increments of 0.1 to a maximum of 95%; r = 0.5 for assimilation curves in figures a, b and c. For Figure 12 d, various r (assimilation rate/crystallization rate) values were considered by using local average upper crust (LUC; Mason et al. 1996) suggesting lower assimilation rate for magmas <12 Ma. All mentioned compositions are given in Supplemental online table S2.2. Symbols as in* Figures 3, 5 and 9
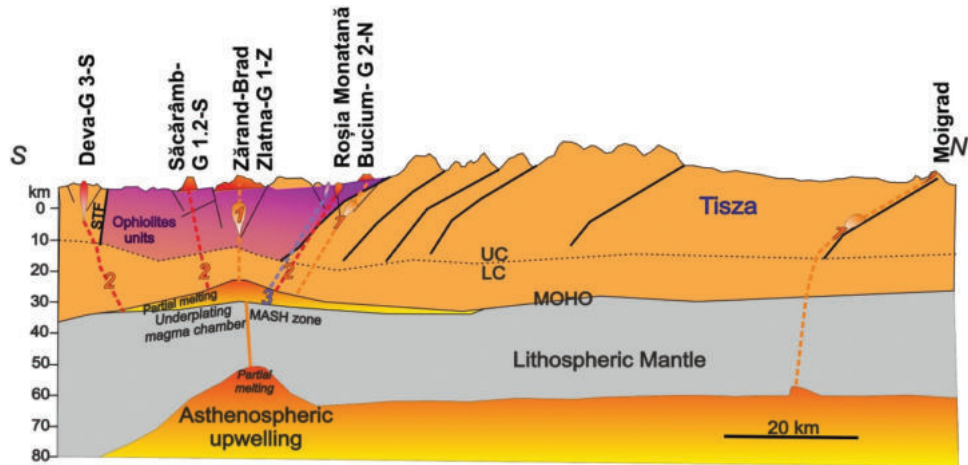

Figure 13. *Geodynamic interpretation of magma genesis and evolution in the Apuseni Mts. on a 140 km S-N profile between Deva and Moigrad (the profile line is shown in* Figure 1b*). The discussed basin/sub-basins are shown, while the labels (1, 2, 3) represent the three evolutionary stages discussed in the text. STF-South Transylvania fault system, UC-upper crust, LC-lower crust.*

Mts. This scenario assumes an important role for crustal break-up during extreme block rotations (~70°) starting at ~14 Ma (Roşu *et al*. 2004), closely related to extension in the Zărand-Békes basin system (Tari *et al*. 1999; Csontos and Vörös 2004; Balázs *et al*. 2016). The extension and simultaneous convective asthenospheric

upwelling may suggest increased heating and further melting of an upper lithospheric mantle/crustal source and the development of an underplating magma chamber (MASH zone model; Figure 13); however, this hypothesis requires further evidence.

The new model adopted here assumes that the primitive magmas formed either by partial melting of asthenospheric mantle, or were generated via partial melting of a hydrous lithospheric mantle (via increased heating), or mixing of melts of these sources. This magma system stalled in an underplated magma chamber (MASH zone) (Figure 13). The mantle-derived magma and increased heating allowed lower crustal partial melting and various extents of mixing with mantle melts. This also was causing weakening of the crust which in turn affected magma ascent and emplacement (Figure 13). We have divided the magmatic evolution into three stages as follows:

(1) In the initial stage (>12 Ma) following initiation of rifting, magmas were emplaced within the main Zărand-Brad-Zlatna graben and some minor in the Roşia Montana – Baia de Arieş sub-basin, giving rise to elongated NNE-SSW oriented intrusions, related to rotation-induced transtensional extension (e.g. Neubauer et al. 2005; Figure 14). In the largest, western part of the Zărand rift basin, the large long-lived composite Bontău volcano (14–10 Ma) was initiated (Figures 1b, 14). As the fault system narrowed towards the east, smaller individual volcanic centres associated with intrusive bodies or multiple-vent volcano-intrusive complexes developed. Such small scattered volcanic centres are also found in Group 2-N. The few remote small intrusions at Moigrad (Figures 1a, 13; North Apuseni Mts.) are difficult to ascribe to the underplated magma chamber below the Zărand basin (ca. 90 km distance). The specific geochemical characteristics (Figure 4 a, b), its time emplacement (~12.4 Ma), and its position between the typical and high Sr/Y rocks may suggest a local asthenospheric disturbance at the end of the regional clockwise rotation movements (Figure 13). Partial melting of an asthenosphere source followed by fractionation and assimilation in the upper crust can be suggested.

(2) The second stage (<12 Ma) suggests a change of the tectonic system to a NW-SE compressional/transpressional one (Neubauer et al. 2005), related to the end of rotation and collision initiation in the East Carpathians (e.g. Maţenco and Bertotti 2000). This led to formation of the wedge-like sub-basins of Caraci (Group 1.1-C) and Săcărâmb (Group 1.2-S) at the southern part of the Zărand-Brad-Zlatna basin (Group 1-Z) (Figure 14) and the generation/rejuvenation of the smaller sub-basins to the north and south of the Săcărâmb

(Group 1.2-S), i.e. the sub-basins at Roşia Montană–Baia de Arieş–Bucium (Group 2-N) and Deva (Group 3-S).

(3) The end of the magmatic activity (~8–7 Ma) was limited to the Roşia Montană–Baia de Arieş–Bucium sub-basin, with eruption of the Detunata basaltic andesites (Group 2-N).

8. Conclusions

The review of published and new data presented in this study suggests a lower crustal origin followed by AFC in the upper crust for the Roşia Montana andesite and dacites (Group 2-N > 12 Ma), an eclogitic origin for the garnet-bearing dacites that show low Zr/Hf and the highest Nb/Zr (Group 1-Z), and an upper mantle-lower crustal origin for the Group 1.1-C rocks along with fractional crystallization ± assimilation and mixing.

Petrographic, geochemical, and isotopic data indicate continuous open-system evolution between 14.5 and 7 Ma of a parental mantle- and/or crustal-derived magma in the deeper parts of the crust (DePaolo 1981; 'MASH zone' of Hildreth and Moorbath 1988) that experienced fractional crystallization and magma mixing processes, as well as assimilation of the upper crust. The high-Sr/Y rocks in the Apuseni Mts., which were previously considered to reflect an adakite-like magma derived from a mantle source that was metasomatized during an earlier subduction event (Roşu et al. 2004; Harris et al. 2013), seems to be associated with both source contamination (upper mantle/lower crust) and differentiation and contamination of mantle/lower crust-derived calc-alkaline melts in the upper crust. The experiments of Qian and Herman (2013) that produced adakite-like rocks from hydrated mafic lower crust at 800–950°C and 10–12.5 kbar support the possibility of generation of high Sr/Y magma at ~35 km depth.

The proposed Miocene evolution in the Apuseni Mts. can be summarized as follows:

1. Between 14.6 and ~12 Ma, normal calc-alkaline magmas were generated in the Zărand-Brad-Zlatna basin (Group 1-Z samples), the Roşia Montană-Baia de Arieş-Bucium sub-basin (Group 2-N rocks) and, independently at Moigrad via lower crustal/uppermost mantle melting, at the initiation of an underplated magma chamber formed through extension via block rotation. Its origin may have been related either to asthenospheric partial melting or to melting of the upper lithospheric mantle via heat from mantle asthenospheric upwelling, or even mixing of such melts. Lower crustal partial melting and mixing with mantle melts occurred. We assume that fractional crystallization started at depths near the base of the crust that contain a certain amount of Sr (an incompatible element that entered the
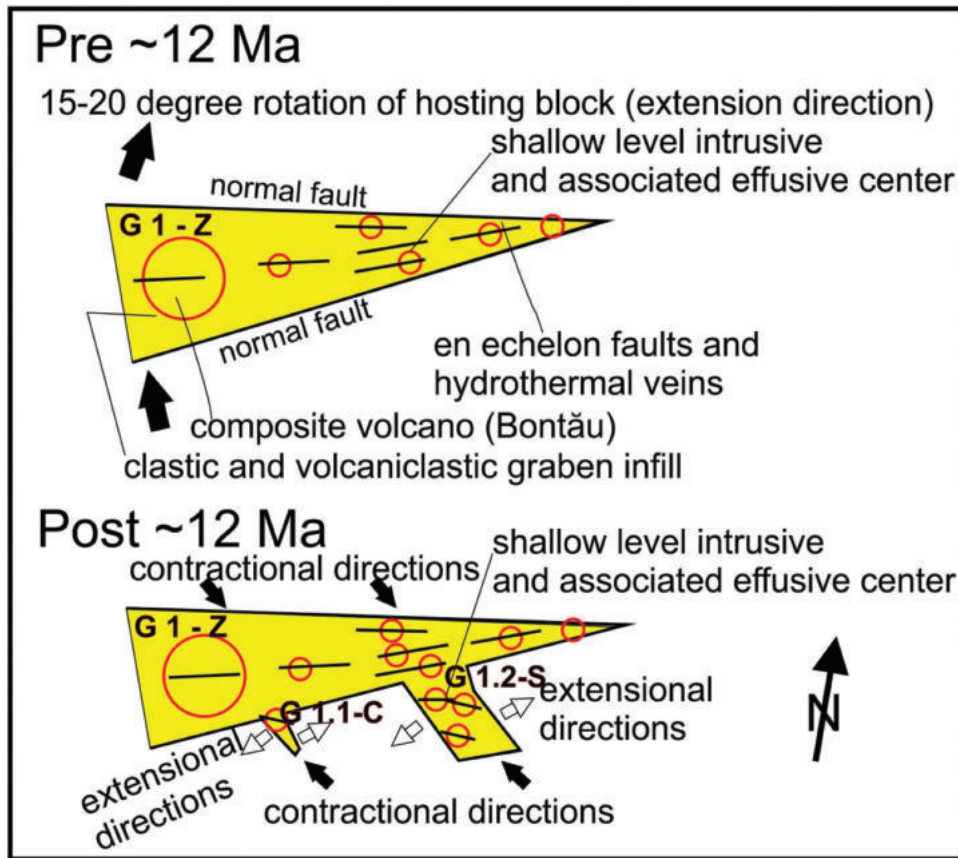
Figure 14. *Simplified map-view showing extension model for the Zărand-Brad-Zlatna- (Group 1-Z) basin, suggesting geodynamic control in an intra-continental oblique rift setting as a result of block rotational extension in the first phase (pre 12 Ma), followed by a NW-SE compressional/transpressional system at post 12 Ma with generation of the wedge-shaped Caraci (Group 1.1-C) and Săcărâmb (Group 1.2-S) sub-basins; Red circles represent volcanic edifices (modified after Neubauer et al. 2005).*

liquid phase; Figure 10). Since all the rocks of the Groups 1-Z and 2-N ranging from basaltic andesites to andesites show constant Sr content (260–340 ppm and 200–250 ppm, respectively) the lowest in the Apuseni region, this may represent the highest MOHO depth according to the crustal thickness beneath the main graben system (<30 km at the present time). The lowest Sr content of the Group 2-N could also be connected to the local lower crust source (Figure 7c, d). Further differentiation and assimilation occurred in upper crustal magma chambers forming magmas up to dacite compositions.

2. After ~12 Ma, typical calc-alkaline magmas continued to erupt in the western part of Zărand-Brad-Zlatna basin (Group 1-Z Bontău volcano) and began in the Caraci sub-basin (Group 1.1-C rocks). These show a dominant mantle origin and a similar Sr content as before ~12 Ma (300–400 ppm). The key magmatism generated high-Sr/Y magmas in all the other small sub-basins (Roşia Montană – Baia de Arieş area and Deva basins producing magmas in Groups 2-N, 1.2-S, and 3-S)

via amphibole/clinopyroxene fractionation ± contamination in crustal magma chambers rich in volatiles, showing a complex mixing between mantle and crustal sources. Higher Sr content characterizes Groups 2-N, 1.2-S (~600 ppm, as dominant) and is highest in the Group 3-S (~1250 ppm, as lowest) that infers a deeper differentiation at the base of lower crust (Figure 10a, b) in accordance with suggested geophysical models (32–35 km). The anomalous high-Sr of the Group 3-S may even suggest generation at a deeper MOHO (~35 km) which may imply a larger volume of crustal melts (amphibolite lithologies) in their source. Further specific contamination of small volume andesite lithologies (high Sr, Ba) of Groups 2-N, 1.2-S occurred in upper crustal magma chambers.

3. Small-volume basaltic andesites (Group 2-N) at ~7–8 Ma in the Roşia Montană – Baia de Arieş sub-basin, which record the last of the Miocene magmatism, may suggest a more primitive mantle-derived magma in the trend of high-Sr/Y calc-alkaline magmas. Their Sr content (~600

ppm) is in the range of Groups 2-N, 1.2-S suggesting a similar depth generation (32–35 km) if the MOHO depth has not changed greatly since Miocene times.

Highlights:

-This review includes all the petrographic types of the Miocene magmatic rocks in the Apuseni Mts;

Additionally, the local Pleistocene alkali-basalts are shown in the diagram for comparison;

-A time-dependent compositional shift indicates Assimilation-Fractional-Crystallization (AFC) processes in two tectonic stages;

-The Miocene extensional model, during collision/post-collision in the East Carpathians, explains the

magma generation processes in a regional context.

Acknowledgments

Disclosure statement

The authors declare that they have not known competing financial interests or personal relationships that could have looked to influence the work reported in this paper.

Funding

ORCID

Ioan Seghedi http://orcid.org/0000-0001-7381-7802
Theodoros Ntaflos http://orcid.org/0000-0001-6665-5868
Zoltan Pécskay http://orcid.org/0000-0002-3571-9352
Cristian Panaiotu http://orcid.org/0000-0001-9332-8926
Viorel Mirea http://orcid.org/0000-0002-4671-7889
Hilary Downes http://orcid.org/0000-0002-2025-162X

References

Bach, P., Smith, I.E.M., and Malpas, J.G., 2012, The Origin of Garnets in Andesitic Rocks from the Northland Arc, New Zealand, and their Implication for Sub-arc Processes: Journal of Petrology, v. 53(6), 1169–1195. 10.1093/petrology/egs012.

Bala, A., Dănila, D.-T., Tătaru, D., and Grecu, B., 2017, Crustal Models Assessment in Western Part of Romania Employing Active Seismic and Seismologic Methods. IOP Conf. Series: Earth and Environmental Science 95 (2017) 032026. doi:10.1088/1755-1315/95/3/032026.

Balázs, A., Burov, E., Maţenco, L., Vogt, K., Francois, T., and Cloetingh, S., 2017, Symmetry during the syn-and post-rift evolution of extensional back-arc basins: The role of inherited orogenic structures: Earth and Planetary Science Letters, v. 462, 86–98. 10.1016/j.epsl.2017.01.015.

Balázs, A., Maţenco, L., Magyar, I., Horváth, F., and Cloetingh, S., 2016, The link between tectonics and sedimentation in back-arc basins: New genetic constraints from the analysis of the Pannonian Basin: Tectonics, v. 35, 1526–1559. 10.1002/2015TC004109

Balintoni, I., 1994, Structure of the Apuseni Mountains. ALCAPA II, Field Guidebook: p. 51–58.

Balintoni, I., 1997, Geotectonica Terenurilor Metamorfice din Romania. Ed. Carpatica, C.-N. Romania, 176. p. (in Romanian). Carpatica.

Balintoni, I., Balica, C., Ducea, M.N., Zaharia, L., Chen, F.K., Cliveti, M., Hann, H.P., Li, L.Q., and Ghergari, L., 2010, Late Cambrian–Ordovician northeastern Gondwanan terranes in the basement of the Apuseni Mountains, Romania: Journal of the Geological Society, v. 167, 1131–1145. 10.1144/0016-76492009-156.

Balintoni, I., and Vlad, S., 1998, Tertiary magmatism in the Apuseni Mountains and related tectonic setting. Studia Univ. Babeş-Bolyai, Geologie IX, 1–11.

Berza, T., Constantinescu, E., and Vlad, S.N., 1998, Upper Cretaceous magmatic series and associated mineralisation in the Carpathian–Balkan Orogen: Resource Geology, v. 48 (4), 291–306. 10.1111/j.1751-3928.1998.tb00026.x.

Bleahu, M., Lupu, M., Patrulius, D., Bordea, S., Ştefan, A., and Panin, S., 1981, The structure of the Apuseni Mountains. Carp. Balk. Geol. Assoc., XII Congr., Guide to Excursion B3, Inst. Geol. Geophys., Bucharest.

Bortolotti, V., Marroni, M., Nicolae, I., Pandolfi, L., Principi, G., and Saccani, E., 2002, Geodynamic implications of Jurassic ophiolites associated with island-arc volcanics, South Apuseni Mountains, western Romania: International Geology Review, v. 44, 938–955. 10.2747/0020-6814.44.10.938.

Boştinescu, S., and Savu, H., 1996, On the high Ba and Sr Deva andesites from the Mureş couloir: Rom. J. Petrology, v. 77, 97–106, Bucharest.

Brunner, M., Müller, L., von Quadt, A., Peytcheva, I., Halga, S., Ruff, R., Tămaş, C, C., and Ivăşcanu, P., 2018, Geochronology and geo-chemistry of zircons from the Rovina Valley/Stănija and Certez deposits – And implications for the Miocene magmatism in the Apuseni Mountains (Romania): Constraints from LA-ICPMS/TIMS dating, trace and REE geo-chemistry of zircons and whole rock studies. XXI International Congress of the Carpathian Balkan Geological

Association (CBGA). University of Salzburg Salzburg (Austria). September 10–13, 2018, Abstracts.

Carr, M., 2010, IGPET. software program. Terra Softa Inc., 155 Emerson RD., Somerset, NJ, 08873.

Chapman, J.B., Ducea, M.N., Profeta, L., and DeCelles, P.G., 2015, Tracking changes in crustal thickness during orogenic evolution with Sr/Y; an example from the Western: U.S. Cordillera. Geology, v. 43, 919–923.

Chung, S.L., Chu, M.F., Zhang, Y.Q., Xie, Y.W., Lo, C.H., Lee, T.Y., Lan, C.Y., Li, X.H., Zhang, Q., and Wang, Y.Z., 2005, Tibetan tectonic evolution inferred from spatial and temporal variations in post-collisional magmatism: Earth-Science Reviews, v. 68, 173–196. 10.1016/j.earscirev.2004.05.001.

Csontos, L., 1995, Tertiary tectonic evolution of the Intra-Carpathian area: A review: Acta Volcanologica, v. 7, 1–13.

Csontos, L., Márton, E., Worum, G., and Benkovics, I., 2002, Geodynamics of SW-Pannonian inselbergs (Mecsek and Villány Mts, SW Hungary): Inference from complex structural analysis, in Neotectonics and surface processes: The Pannonian Basin and Alpine-Carpathian system, Stephan Mueller spec. Publ. Ser., vol. 3, edt. S. A. P. L. Cloetingh et al., p. 1-19, Eur. Geosci. Union, Munich. Germany.

Csontos, L. and Nagymarosy, A., 1998, The Mid-Hungarian line; a zone of repeated tectonic inversions. Tectonophysics v. 297, 51–71.

Csontos, L., and Vörös, A., 2004, Mesozoic plate tectonic reconstruction of the Carpathian region: Palaeogeography, Palaeoclimatology, Palaeoecology, v. 210, 1–56.

Dallmeyer, R.D., Pană, D.I., Neibauer, F., and Erdmer, P., 1999, Tectonothermal evolution of the Apuseni mountains, Romania: Resolution of variscan versus alpine events with 40Ar/39 Ar ages: The Journal of Geology, v. 107, 329–352. 10.1086/314352.

Davidson, J., 1998, Strontium in igneous rocks. In: Geochemistry. Encyclopedia of earth science. Springer, Dordrecht. 10.1007/1-4020-4496-8_300.

Davidson, J., Turner, S., Handley, H., Macpherson, C. and Dosseto, A., 2007, An amphibole 'sponge' in arc crust? Geology v. 35, 787–790.

Davidson, J., Turner, S., and Plank, T., 2013, Dy/Dy*: Variations arising from mantle sources and petrogenetic processes: Journal of Petrology, v. 54(3), 525–537. 10.1093/petrology/egs076.

DePaolo, D.J., 1981, Trace element and isotopic effects of combined wallrock assimilation and fractional crystallization: Earth planet: Science Letters, v. 53, 189–202.

Dilek, Y., and Altunkaynak, Ş., 2009, Geochemical and temporal evolution of Cenozoic magmatism in western Turkey: Mantle response to collision, slab break-off, and lithospheric tearing in an orogenic belt. Van Hinsbergen, D.J.J., Edwards, M.A., and Govers, R., eds. Collision and Collapse at the Africa–Arabia–Eurasia Subduction zone. Geol. Society: London, Special Publications, Vol. 311. 213–233.

Dinu, C., Calotă, C., Mocanu, V., and Ciulavu, D., 1991, Geotectonic setting and the particular structural features of the Beiuş basin, on the basis of geological and geophysical data synthesis: Revue Roumaine de Geophysique, v. 35, 77–87.

Downes, H., Seghedi, I., Szakács, A., Dobosi, G., James, D.E., Vaselli, O., Rigby, I.J., Ingram, G.A., Rex, D., and Pécskay, Z., 1995, Petrology and geochemistry of the late Tertiary/ Quaternary mafic alkaline volcanism in Romania: Lithos, v. 35, 65–81. 10.1016/0024-4937(95)91152-Y.

xxxx

Eiler, J.M., Crawford, A., Elliot, T., Farley, K.A., Valley, J.W., and Stolper, E.M., 2000, Oxygen isotope geochemistry of oceanic-arc lavas: Journal of Petrology, v. 41, 229–256. 10.1093/petrology/41.2.229.

Ene, V.V., Smith, D.J., Tapster, S., Roşu, E., Munteanu, M., and Naden, J., 2019, Spatial and temporal evolution of arc-like post-subduction magmas: Apuseni, Romania. Barcelona (Spain). Goldschmidt 2019. Abstract.

Ersoy, E.Y., and Palmer, M.R., 2013, Eocene–Quaternary magmatic activity in the Aegean: Implications for mantle metasomatism and magma genesis in an evolving orogeny: Lithos, v. 180-181, 5–24. 10.1016/j.lithos.2013.06.007.

Fodor, L., Csontos, L., Bada, G., Györfi, I., and Benkovics, L., 1999, Tertiary tectonic evolution of the Pannonian Basin system and neighbouring orogens; a new synthesis of palaeostress data. The Mediterranean basins; tertiary extension within the alpine orogen.Durand, B., Jolivet, L., Horvath, F., and Seranne, M., eds. Geol. Soc. Spec. Publ, Vol. 156. 295–334.

Gallhofer, D., 2015, Magmatic geochemistry and geochronology in relation to the geodynamic and metallogenic evolution of the Banat Region and the Apuseni Mountains of Romania. PhD Thesis. ETH Zürich, Diss. No. 22888, 145.

Gallhofer, D., Quadt, A., Peytcheva, I., Schmid, S.M., and Heinrich, C.A., 2015, Tectonic, magmatic, and metallogenic evolution of the Late Cretaceous arc in the Carpathian– Balkan orogen: Tectonics, v. 34(9), 1813–1836. 10.1002/2015TC003834.

Gallhofer, D., von Quadt, A., Schmid, S.M., Guillong, M., Peytcheva, I., and Seghedi, I., 2017, Magmatic and tectonic history of Jurassic ophiolites and associated granitoids from the South Apuseni Mountains (Romania): Swiss Journal of Geosciences, v. 110, 699–719. 10.1007/s00015-016-0231-6.

Ghiţulescu, T.P., and Socolescu, M., 1941, Étude géologique et minière des Monts Metallilifères (Quadrilatère aurifère et régions environnantes): An. Inst. Geol, v. 21, 181–464.

Haas, J. and Péró, C., 2004. Mesozoic evolution of the Tisza Mega-unit. Int. J. Earth Sci. v. 93, 297–313.

Harris, C.R., Pettke, T., Heinrich, C.A., Roşu, E., Woodland, S., and Fry, B., 2013, Tethyan mantle metasomatism creates subduction geochemical signatures in non-arc Cu–Au–Te mineralizing magmas: Apuseni Mountains (Romania). Earth and Planetary Science Letters, v. 366, 122–136. 10.1016/j.epsl.2013.01.035.

Hawkesworth, C.J., Gallagher, K., Hergt, J.M., and McDermott, F., 1993, Mantle and slab contributions in arc magmas: Annual Reviews of Earth Planetary Science, v. 21, 175–204. 10.1146/annurev.ea.21.050193.001135.

Hildreth, W., and Moorbath, S., 1988, Crustal contributions to arc magmatism in the Andes of central Chile: Contributions to Mineralogy and Petrology, v. 98(4), 455–489. 10.1007/BF00372365.

Hindson, T., 2009, The geology and geochemical signature of the Talagiu Complex, Apuseni Mountains, NW Romania. Diss. for Master of Geology, Univ. of Southampton. 71.

Hoeck, V., Ionescu, C., Balintoni, I., and Koller, F., 2009, The Eastern Carpathians 'ophiolites' (Romania): Remnants of a Triassic ocean: Lithos, v. 108, 151–171. 10.1016/j.lithos.2008.08.001.

Holder, D.S., 2016, Geological and geochemical controls for epithermal Au-Ag-Te (Pb-Zn) mineralisation at Coranda-Hondol and the Brad-Săcărâmb basin mineral district of western Romania. PhD thesis, Kingston University, 376 p.

Horváth, F., 1993, Towards a mechanical model for the formation of the Pannonian basin: Tectonophysics, v. 226, 333–357. 10.1016/0040-1951(93)90126-5.

Horváth, F., Bada, G., Szafian, P., Tari, G., Adam, A., and Cloetingh, S., 2006, Formation and deformation of the Pannonian Basin: Constraints from observational data: Geological Society, London, Memoirs, v. 32(1), 191–206. 10.1144/GSL.MEM.2006.032.01.11.

Horváth, F., Musitz, B., Balázs, A., Végh, A., Uhrin, A., Nádor, A., Koroknai, B., Pap, N., Tóth, T., and Wórum, G., 2015, Evolution of the Pannonian Basin and its geothermal resources: Geothermics, v. 53, 328–352. 10.1016/j.geothermics.2014.07.009.

Hoskin, P.W.O., and Schaltegger, U., 2003, The composition of zircon and igneous and metamorphic petrogenesis: Reviews in Mineralogy & Geochemistry, v. 53(1), 27–62. 10.2113/0530027.

Hu, F., Ducea, M.N., Liu, S., and Chapman, J.B., 2017, Quantifying Crustal thickness in continental collisional belts: Global perspective and a geologic application: Scientific Reports, v. 7, 7058. 10.1038/s41598-017-07849-7

Ianovici, V., Borcoş, M., Bleahu, M., Patrulius, D., Lupu, M., Dimitrescu, R., and Savu, H., 1976, Geology of the Apuseni mountains. Ed. Acad. Rep. Soc, România, 631 (in Romanian).

Ianovici, V., Giuşcă, D., Ghiţulescu, T.P., Borcoş, M., Lupu, M., Bleahu, M., and Savu, H., 1969, Geological evolution of the Metaliferi Mountains. Ed. Acad. Rep. Soc, România, 741 (in Romanian).

Ilie, D.M., 1958, Structure geologique de la depression d'Abrud: An. Com. Geol, v. XXIV-XXV, 217–239.

Ionescu, C., Hoeck, V., Tomek, C., Koller, F., Balintoni, I., and Beşuţiu, L., 2009, New insights into the basement of the Transylvanian Depression (Romania): Lithos, v. 108, 172–191. 10.1016/j.lithos.2008.06.004

Jicha, B., Garret L. H., R., Johnson, K.M., Hildreth, W., Beard, B.L., Shirey, S.B., and Valley, J.W., 2009, Isotopic and trace element constraints on the petrogenesis of lavas from the Mount Adams volcanic field, Washington: Contributions to Mineralogy and Petrology, v. 157, 189–207. 10.1007/s00410-008-0329-6

Jude, R., Tabaciu-Borcea, M., and Ionescu, O., 1973, Geological and petrographical study of the effusive rocks from Caraciu volcano (Metaliferi Mountains) (In Romanian): An. Inst. Geol, v. 40, 8–69.

Kendrick, J., and Yakymchuk, C., 2020, Garnet fractionation, progressive melt loss and bulk composition variations in anatectic metabasites: Complications for interpreting the geodynamic significance of TTGs: Geoscience Frontiers, v. 11, 745–763. 10.1016/j.gsf.2019.12.001

Kouzmanov, K., Pettke, T., Heinrich, C., Riemer, S., Ivăşcanu, P., and Roşu, E., 2003, The porphyry to epithermal transition in a magmatic-hydrothermal system: Valea Morii copper–gold deposit, Apuseni Mts, Romania: Mineral Exploration Sustainable Development, v. 1, p. 303-306.

Kouzmanov, K., von Quadt, A., Peycheva, I., Harris, R.C., Heinrich, C.A., Roşu, E., and Ivăşcanu, P.M., 2007, Miocene magmatism and ore formations in the South Apuseni Mountains, Romania: New genetic and timing constraints. Proceedings of the Ninth Biennal SGA Meeting, Dublin 2007, p. 865–868.

Kouzmanov, K., von Quadt, A., Peytcheva, I., Harris, C., Heinrich, C., Roşu, E., and O'Connor, G., 2005, Roşia Poieni porphyry Cu–Au and Roşia Montana epithermal Au–Ag deposits, Apuseni Mountains, Romania: Timing of magmatism and related mineralisation: Geochem. Miner. Petrol, v. 42, 113–117.

Kouzmanov, K., von Quadt, A., Peytcheva, I., Heinrich, C.A., Pettke, T., and Roşu, E., 2006, Geochemical and time constraints on porphyry ore formation in the Barza magmatic complex, Apuseni Mountains, Romania. In: Proceedings of the IGCP Project 486 Field Workshop, Izmir, Turkey.

Krézsek, C., and Bally, A., 2006, The Transylvanian Basin (Romania) and its relation to the Carpathian fold and thrust belt: Insights in gravitational salt tectonics, Mar: Marine and Petroleum Geology, v. 23, 405–442. 10.1016/j.marpetgeo.2006.03.003

Le Bas, M.J., Le Maitre, R.W., Streckeisen, A., and Zanettin, B., 1986, A chemical classification of volcanic rocks based on the total alkali-silica diagram: Journal of Petrology, v. 27, 745–750. 10.1093/petrology/27.3.745.

Lexa, J., Seghedi, I., Németh, K., Szakács, A., Konečný, V., Pécskay, Z., Fülöp, A., and Kovacs, M., 2010, Neogene–Quaternary volcanic forms in the Carpathian–Pannonian Region: A review: Cent. Eur. J. Geosci, v. 2(3), 207–270.

Linzer, H.G., 1996, Kinematics of retreating subduction along the Carpathian arc, Romania: Geology, v. 24(2), 167–170. 10.1130/0091-7613(1996)024<0167:KORSAT>2.3.CO;2.

Lustrino, M., Duggen, S., and Rosenberg, C.L., 2011, The central-western Mediterranean: Anomalous igneous activity in an anomalous collisional tectonic setting: Earth-Science Reviews, v. 104, 1–40. 10.1016/j.earscirev.2010.08.002.

Mason, P., Downes, H., Thirlwall, M.F., Seghedi, I., Szakács, A., Lowry, D., and Mattey, D., 1996, Crustal assimilation as a major petrogenetic process in the east Carpathian Neogene and Quaternary continental margin arc, Romania: Journal of Petrology, v. 37, 927–959. 10.1093/petrology/37.4.927.

Mason, P.R.D., Seghedi, I., Szakács, A., and Downes, H., 1998, Magmatic constraints on geodynamic models of subduction in the Eastern Carpathians, Romania: Tectonophysics, v. 297, 157–176. 10.1016/S0040-1951(98)00167-X.

Maţenco, L., 2017, Tectonics and Exhumation of Romanian Carpathians: Inferences from kinematic and thermochronological studies, 15-56; chapter 2. Rădoane, M., and Vespremeanu-Stroe, A., eds. Landform dynamics and evolution in Romania, Springer Geography. 10.1007/978-3-319-32589-7_2

Maţenco, L., and Bertotti, G., 2000, Tertiary tectonic evolution of the external East Carpathians (Romania): Tectonophysics, v. 316, 255–286. 10.1016/S0040-1951(99)00261-9.

Maţenco, L., Krézsek, C., Merten, S., Schmid, S., Cloetingh, S., Andriessen, P., 2010, Characteristics of collisional orogens with low topographic build-up: an example from the Carpathians. Terra Nova v. 22, 155–165.

McNab, F., Ball, P.W., Hoggard, M.J., and White, N.J., 2018, Neogene uplift and magmatism of Anatolia: Insights from drainage analysis and basaltic geochemistry: Geochemistry, Geophysics, Geosystems, v. 19, 175–213. 10.1002/2017GC007251

Merten, S., Maţenco, L., Foeken, J.P.T., and Andriessen, P.A.M., 2011, Toward understanding the postcollisional evolution of an orogen influenced by convergence at adjacent plate margins: Late Cretaceous-Tertiary thermotectonic history of the Apuseni Mountains: Tectonics, v. 30(6), TC6008. 10.1029/2011TC002887.

Neubauer, F., Lips, A., Kouzmanov, K., Lexa, J., and Ivăşcanu, P., 2005, Subduction, slab detachment and mineralization: The Neogene in the Apuseni Mountains and Carpathians: Ore Geology Reviews, v. 27, 13–44. 10.1016/j.oregeorev.2005.07.002.

Nicolae, I., and Saccani, E., 2003, Petrology and geochemistry of the late Jurassic calc-alkaline series associated to Middle Jurassic ophiolites in the South Apuseni Mountains, Romania, Schweiz: Min. Petr. Mitt, v. 83, 81–96.

Niu, Y., Zhao, Z., Zhuc, D.-C., and Mo, X., 2013, Continental collision zones are primary sites for net continental crust growth - A testable hypothesis: Earth-Science Reviews, v. 127, 96–110. 10.1016/j.earscirev.2013.09.004.

xxx

Pană, D., Heaman, L.M., Creaser, R.A., and Erdmer, P., 2002, Pre-alpine crust in the Apuseni Mountains, Romania: Insights from Sm–Nd and U–Pb data: The Journal of Geology, v. 110(3), 341–354. 10.1086/339536.

Panaiotu, C., 1998, Paleomagnetic constraints on the geodynamic history of Romania. Reports on Geodesy 7. Warsaw University of Technology, Warsaw, 205–216.

Pătraşcu, S., Panaiotu, C., Şeclaman, M., and Panaiotu, C.E., 1994, Timing and rotational motions of Apuseni Mountains, Romania: Palaeomagnetic data from Tertiary magmatic rocks: Tectonophysics, v. 233, 163–176. 10.1016/0040-1951(94)90239-9.

Pearce, J.A., 2008, Geochemical fingerprinting of oceanic basalts with applications to ophiolite classification and the search for Archean oceanic crust: Lithos, v. 100, 14–48. 10.1016/j.lithos.2007.06.016.

Peccerillo, A., and Taylor, S.R., 1976, Geochemistry of Eocene calc-alkaline volcanic rocks from the Kastamonu Area: Contributions to Mineralogy and Petrology, v. 58, 63–81. 10.1007/BF00384745.

Pécskay, Z., Edelstein, O., Seghedi, I., Szakács, A., Kovacs, M., Crihan, M., and Bernad, A., 1995, K-Ar datings of the Neogene-Quaternary calc-alkaline volcanic rocks in Romania: Acta Vulcanologica, v. 7, 53–63.

Pécskay, Z., Lexa, J., Szakács, A., Seghedi, I., Balogh, K., Konecný, V., Zelenka, T., Kovacs, M., Póka, T., Fülöp, A., Márton, E., Panaiotu, C., and Cvetković, V., 2006, Geochronology of Neogene magmatism in the Carpathian arc and intra-Carpathian area: Geological Carpathica, v. 57 (6), 511–530.

xxxx

Petford, N., and Atherton, M., 1996, Na-rich partial melts from newly underplated basaltic crust: The Cordillera Blanca batholith, Peru, J: Journal of Petrology, v. 37, 1491–1521. 10.1093/petrology/37.6.1491.

Prelević, D. and Seghedi, I., 2013, Magmatic response to the post-accretionary orogenesis within Alpine–Himalayan belt—preface. Lithos v. 181, 1–4.

Profeta, L., Ducea, M.N., Chapman, J.B., Paterson, S.R., Gonzales, S.M.H., Kirsch, M., et al. 2015, Quantifying crustal thickness over time in magmatic arcs: Scientific Reports, v. 5 (1), 1–7. 10.1038/srep17786.

Qian, Q., and Herman, J., 2013, Partial melting of lower crust at 10–15 kbar: Constraints on adakite and TTG formation: Contributions to Mineralogy and Petrology, v. 165(6), 1195–1224. Doi: 10.1007/s00410-013-0854-9.

Rabayrol, F., Hart, C.J.R., and Thorkelson, D.J., 2019, Temporal, spatial and geochemical evolution of late Cenozoic post-subduction magmatism in central and eastern Anatolia, Turkey: Lithos, v. 336–337, 67–96. Doi: 10.1016/j.lithos.2019.03.022

Reiser, M.K., Schuster, R., Spikings, R., Tropper, P., and Fügenschuh, B., 2016, From nappe stacking to exhumation: Cretaceous tectonics in the Apuseni Mountains (Romania): International Journal of Earth Science (Geol. Rundsch.), 10.1007/s00531-016-1335-y.

xxxx

Richards, J.P., and Kerrich, R., 2007, Special paper: Adakite-like rocks: Their diverse origins and questionable role in metallogenesis: Economic Geology, v. 102(4), 537–576. 10.2113/gsecongeo.102.4.537.

Rollinson, H.R., 1993, Using geochemical data: Evaluation, presentation, interpretation: Longman Scientific & Technical, 352.

Roşu, E., Pécskay, Z., Ştefan, A., Popescu, G., Panaiotu, C., and Panaiotu, C.E., 1997, The evolution of the Neogene volcanism in the Apuseni Mountains (Romania): Constraints from new K/Ar data: Geologica Carpathica, v. 48(6), 353–359.

Roşu, E., Seghedi, I., Downes, H., Alderton, D.H.M., Szakács, A., Pécskay, Z., Panaiotu, C., Panaiotu, C.E., and Nedelcu, L., 2004, Extension-related Miocene calc-alkaline magmatism in the Apuseni Mountains, Romania: Origin of magmas: Swiss Bulletin of Mineralogy and Petrology, v. 84(1–2), 153–172.

Rudnick, R.L., and Gao, S., 2003, Composition of the Continental Crust: Treatise on Geochemistry, v. 3, 1–64.

Saccani, E., Nicolae, I., and Tassinari, R., 2001, Tectono-magmatic setting of the ophiolites from the South Apuseni Mountains (Romania): Petrological and geochemical evidence: Ofioliti, v. 26, 9–22.

Săndulescu, M., 1984, Geotectonics of Romania. Ed. Tehnică, Bucureşti. 366. (in Romanian).

Săndulescu, M., 1988, Cenozoic tectonic history of the Carpathians. The Pannonian Basin: A study in basin evolution.Royden, L., and Horvath, F., eds. AAPG Memoir, Vol. 45. 17–25.

Săndulescu, M., 1988, Cenozoic tectonic history of the Carpathians. Am. Assoc. Pet. Geol. Mem. v. 45, 17–25.

Savu, H., 1996, A comparative study of the ophiolites obducted from two different segments of the Mures ocean "Normal" median ridge (Romania): Romanian Journal of Petrology, v. 77, 46–60.

Schmid, S.M., Bernoulli, D., Fügenschuh, B., Maţenco, L., Schefer, S., Schuster, R., Tischler, M., and Ustaszewski, K., 2008, The Alpine-Carpathian-Dinaridic orogenic system: Correlation and evolution of tectonic units: Swiss Journal of Geosciences, v. 101(1), 139–183. 10.1007/s00015-008-1247-3.

Schmid, S.M., Fügenschuh, B., Kounov, A., Maţenco, L., Nievergelt, P., Oberhänsli, R., Pleuger, J., Schefer, S., Schuster, R., Tomljenović, B., Ustaszewski, K., and Van Hinsbergen., D.J.J., 2020, Tectonic units of the Alpine collision zone between Eastern Alps and western Turkey: Gondwana Research, v. 78, 308–374.

Schuller, V., Frisch, W., Danisik, M., Dunkl, I., and Melinte, M.C., 2009, Upper Cretaceous Gosau deposits of the Apuseni Mountains (Romania) - Similarities and differences to the Eastern Alps: Austrian Journal of Earth Science, v. 102, 133–145.

Seghedi, I., Balintoni, I., and Szakács, A., 1998, Interplay of tectonics and Neogene post-collisional magmatism in the Intracarpathian area: Lithos, v. 45, 483–499. 10.1016/S0024-4937(98)00046-2.

Seghedi, I., Bojar, A.-V., Downes, H., Roşu, E., Tonarini, S., and Mason, P.R.D., 2007, Generation of normal and adakite-like calc-alkaline magmas in a non-subductional environment: A Sr-O-H isotopic study of the Apuseni Mountains Neogene magmatic province: Romania Chemical Geology, v. 245, 70–88. 10.1016/j.chemgeo.2007.07.027.

Seghedi, I., and Downes, H., 2011, Geochemistry and tectonic development of Cenozoic magmatism in the Carpathian–Pannonian region: Gondwana Research, v. 20, 655–672. 10.1016/j.gr.2011.06.009.

Seghedi, I., Downes, H., Szakács, A., Mason, P.R.D., Thirlwall, M. F., Roşu, E., Pécskay, Z., Marton, E., and Panaiotu, C., 2004, Neogene-Quaternary magmatism and geodynamics in the Carpathian-Pannonian region: A synthesis: Lithos, v. 72, 117–146. 10.1016/j.lithos.2003.08.006.

xxxx

Seghedi, I., Ntaflos, T., and Pécskay, Z., 2008, The Gătaia Pleistocene lamproite: A new occurrence at the southeastern edge of the Pannonian Basin, Romania: Geological Society London Special Publication, v. 293, 83–100. 10.1144/SP293.5

Seghedi, I., Szakács, A., Roşu, E., Pécskay, Z., and Gmeling, K., 2010, Note on the evolution of a Miocene composite volcano in an extensional setting, Zărand Basin (Apuseni Mts., Romania): Central European Journal of Geosciences, v. 2(3), 321–328.

Sun, -S.-S., and McDonough, W.F., 1989, Chemical and isotopic systematics of oceanic basalts: Implications for mantle composition and processes, Geol: Geological Society, London, Special Publications, v. 42(1), 313–345. 10.1144/GSL.SP.1989.042.01.19.

Sz., H., Downes, H., Kósa, L., Cs., S., Thirlwall, M.F., Mason, P.R.D., and Mattey, D., 2001, Almandine garnet in calcalkaline volcanic rocks of the Northern Pannonian Basin (Eastern–Central Europe): Geochemistry, petrogenesis and geodynamic interpretations: Journal of Petrology, v. 42, 1813–1843. 10.1093/petrology/42.10.1813.

Sz., H., and Lenkey, L., 2007, Genesis of the Neogene to Quaternary volcanism in the Carpathian–Pannonian region: Role of subduction, extension, and mantle plume: Geological Society of America Special Paper, v. 418, 67–90.

Tari, G., Dovenyi, P., Dunkl, I., Horvath, F., Lenkey, L., Ştefănescu, M., Szafian, P., and Toth, T.,1999, Lithospheric structure of the Pannonian basin derived from seismic, gravity and geothermal data. Durand, B., Jolivet, L., Horvath, F., and Serrane, M., eds. The Mediterranean basins: Extension within the Alpine Orogen. Geol. Soc. London Spec. Publ Vol. 156, 215–250.

Tepley, I.I.I., Davidson, F.J., Tilling, R.I, J.P., and Arth, J.G., 2000, Magma mixing, recharge and eruption histories recorded in plagioclase phenocrysts from El Chichón Volcano, Mexico: Journal of Petrology, v. 41, 1397–1411. 10.1093/petrology/41.9.1397.

Tschegg, C., Ntaflos, T., Kiraly, F., and Harangi, S., 2010, High temperature corrosion of olivine phenocrysts in Pliocene basalts from Banat: Romania. Austrian Journal of Earth Sciences, v. 103, 101–110.

Uslular, G., and Gençalioğlu-Kuşcu, G., 2019, Geochemical characteristics of Anatolian basalts: Comment on "Neogene uplift and magmatism of Anatolia: Insights from drainage analysis and basaltic geochemistry" by McNab et al: Geochemistry, Geophysics, Geosystems, v. 20, 530–541. 10.1029/2018GC007533.

Ustaszewski, K., Schmid, S., Fügenschuh, B., Tischler, M., Kissling, E., and Spakman, W., 2008, A map-view restoration of the Alpine–Carpathian–Dinaridic system for the Early Miocene: Swiss Journal of Geosciences, v. 101, 273–294. 10.1007/s00015-008-1288-7.

Van Hinsbergen, D.J.J., Torsvik, T.H., Schmid, S.M., Maţenco, L. C., Maffione, M., Vissers, R.L.M., Gürer, D., and Spakman, W., 2020, Orogenic architecture of the Mediterranean region and kinematic reconstruction of its tectonic evolution since the Triassic: Gondwana Res, v. 81, 79–229.

Van Westrenen, W., Blundy, J.D., and Wood, B.J., 2001, High field strength element/rare earth element fractionation during partial melting in the presence of garnet: Implications for identification of mantle heterogeneities. G3, 2, Paper number 2000GC000133.

Vander Auwera, J., Berza, T., Gesels, J., and Dupont, A., 2015, The Late Cretaceous igneous rocks of Romania (Apuseni Mountains and Banat): The possible role of amphibole versus plagioclase deep fractionation in two different crustal terranes: International Journal of Earth Science (Geol Rundsch), 10.1007/s00531-015-1210-2.

Wenzel, T., Baumgartner, L.P., Brügmann, G.E., Konnikov, E.G. Kislov, E.V., and Orsoev, D.A., 2001, Contamination of mafic magma by partial melting of dolomitic xenoliths: Terra Nova, v. 13, 197–202. 10.1046/j.1365-3121.2001.00340.x.

Zindler, A., and Hart, S., 1986, Chemical geodynamics: Annual Review of Earth and Planetary Sciences, v. 14, 493–571. 10.1146/annurev.ea.14.050186.002425.